View metadata, citation and similar papers at core.ac.uk

brought to you by CORE

provided by Digital Repository @ Iowa State University

IOWA STATE UNIVERSITY
Digital Repository

Retrospective Theses and Dissertations

Iowa State University Capstones, Theses and Dissertations

1966

Calcium sulfate crystallization in phosphoric acid

Ashok Babubhai Amin
Iowa State University

Follow this and additional works at: https://lib.dr.iastate.edu/rtd


Part of the Chemical Engineering Commons

Recommended Citation

Amin, Ashok Babubhai, "Calcium sulfate crystallization in phosphoric acid " (1966). *Retrospective Theses and Dissertations*. 2852.
https://lib.dr.iastate.edu/rtd/2852

This Dissertation is brought to you for free and open access by the Iowa State University Capstones, Theses and Dissertations at Iowa State University Digital Repository. It has been accepted for inclusion in Retrospective Theses and Dissertations by an authorized administrator of Iowa State University Digital Repository. For more information, please contact digirep@iastate.edu.

This dissertation has been
microfilmed exactly as received

66–6973

AMIN, Ashok Babubhai, 1939–

CALCIUM SULFATE CRYSTALLIZATION IN PHOSPHORIC ACID.

Iowa State University of Science and Technology
Ph.D., 1966
Engineering, chemical

University Microfilms, Inc., Ann Arbor, Michigan

CALCIUM SULFATE CRYSTALLIZATION

IN PHOSPHORIC ACID

by

Ashok Babubhai Amin

A Dissertation Submitted to the

Graduate Faculty in Partial Fulfillment of

The Requirements for the Degree of

DOCTOR OF PHILOSOPHY

Major Subject: Chemical Engineering

Approved:

Signature was redacted for privacy.

In Charge of Major Work

Signature was redacted for privacy.

Head of Major Department

Signature was redacted for privacy.

Dean of Graduate College

Iowa State University
Of Science and Technology
Ames, Iowa

1966

TABLE OF CONTENTS

INTRODUCTION

Chemical processes involving crystallization, regardless of whether it is cooling crystallization, salting-out crystallization or reaction crystallization, have seldom been studied systematically because until recently crystallization has been considered as an art rather than a science. Considerable theoretical work has been done recently in studying continuous mixed suspension, mixed product removal (MSMPR) crystallizers (4,16,21,27, 29,30,33). An extensive theoretical study of unsteady state MSMPR crystallizer was done by Randolph and Larson (29). A steady state model of the size distribution was derived in their study, which can be written as follows:

$$n_o = n_o^o \exp(-L/r_o T_o) \qquad (1)$$

where n_o is the steady state population density, n_o^o is the steady state nuclei population density, L is particle diameter, r_o is the steady state growth rate and T_o is the steady state residence time. The population density n is defined as the rate of change of the number of crystals with respect to size in a given crystal distribution. This equation was also derived previously in a less general way by Bransom et al. (4) and Saeman (30). Experimental work based on this model can yield very useful information which may be used to improve operation and control of continuous crystallizers. Application of this model for the study of the processes involving crystallization could bring out important advances.

The process of the present study was the traditional wet-process for phosphoric acid manufacture. This is one of the most complex processes involving crystallization and probably the least studied from the view point of continuous crystallization. The development of wet-process

phosphoric acid manufacture is closely associated with the production of chemical fertilizers. Numerous wet-processes (10,17,31) have been developed over a long period of time. From a chemical point of view they have the common feature that phosphate rock is treated with sulfuric acid resulting in the liberation of phosphoric acid and formation of calcium sulfate in one or more of its crystal forms, followed by separation of the solids from the liquid. One or more of the following reactions take place in the wet-process phosphoric acid production depending upon the process.

$$Ca_{10}F_2(PO_4)_6 + 14\ H_3PO_4 \rightarrow 10\ Ca(H_2PO_4)_2 + 2HF \qquad (2)$$

$$Ca(H_2PO_4)_2 + H_2SO_4 \rightarrow CaSO_4 + 2\ H_3PO_4 \qquad (3)$$

$$Ca_{10}F_2(PO_4)_6 + 10\ H_2SO_4 \rightarrow 10\ CaSO_4 + 6\ H_3PO_4 + 2HF \qquad (4)$$

The problems associated with the crystallization of calcium sulphate created major difficulty when the world's first phosphoric acid plant was established at Biebrich, Germany in 1870, and this position has not changed much even today (37). The wet-process is identified by the type of the calcium sulfate crystals formed, namely, dihydrate, semihydrate or anhydrite. In most of the wet-process plants in the United States calcium sulfate is crystallized as gypsum (dihydrate).

The principal objectives (37) of any phosphoric acid process are to

(1) extract the maximum amount of P_2O_5 from the phosphate rock,

(2) precipitate rapidly filtering and easily washable calcium sulfate crystals,

(3) produce phosphoric acid having as high a concentration as possible,

(4) maintain continuous production over long periods at design capacities

(5) minimize operating labor and maintenance cost,

(6) have safe, clean plant operation with absence of air and stream pollution.

Relatively few plants achieve (37) all these objectives, often because of an insufficient knowledge of fundamental principles.

Very little work has been done in studying the wet-process from the crystallization point of view. The present day problems of wet-process plants fall into the category of mainly crystallization problems. This is so because calcium sulfate is a sparingly soluble salt in phosphoric acid, which makes the growth and nucleation kinetics very unfavorable for good crystallization. Moreover, calcium sulfate crystallizes in different forms and habits depending upon operating conditions. The size of the crystals formed is generally between 0 and 150 microns, with a major portion of the crystals of size less than 40 microns. The filtration and the washing of these fine crystals free of phosphoric acid is the most difficult and economically critical part of the process. Any amount of acid that is retained in the filter cake is lost. This type of loss has been reported to be as high as 10 percent of the theoretical yield.

Most of the wet phosphoric acid produced is used in the production of triple superphosphate and ammonium phosphate. In 1955 U.S. plants produced only 885,000 tons of wet phosphoric acid. The production estimate (24) for 1965 is 2,550,000 tons. Considering this quantity, even a small increase in the recovery of phosphoric acid amounts to significant savings. Commercial processes in use today recover 85 to 95 percent of P_2O_5 in the rock phosphate as phosphoric acid, and the rest generally is lost with the gypsum. In addition to the losses due to poor filtration and washing are

the losses due to unreacted phosphate rock and incorporation of the PO_4 ions in the gypsum crystal structure. Under poor crystallization conditions some of the rock particles become coated with calcium sulfate and are lost in the waste gypsum, as unreacted rock phosphate. Gypsum and dicalcium phosphate have almost identical crystal structures and under poor control, may form a solid solution resulting in a phosphate loss.

It would be desirable to produce phosphoric acid which could be used directly without further concentration of the acid. Wet phosphoric acid is a highly impure, viscous liquid with large amounts of scale forming and corrosive compounds dissolved in it. Increasing the concentration of such an acid has always been a very difficult operation. Wet-processes crystallizing gypsum can produce acid of only 30 to 32 percent P_2O_5 concentration. Further concentration of this acid is necessary for its use. Processes based on semihydrate or anhydrite can produce a higher concentration acid but they have not received proper attention in the past because of the unavailability of suitable materials of construction which resist the higher temperatures that are required. Now with the economically available newer materials of construction a need for a process based on semihydrate crystallization exists. Recently (10) Tennessee Valley Authority has started development of a wet-process which crystallizes calcium sulfate as semihydrate. Unfortunately, in the development of the process, as in the past for gypsum processes, fundamentals of crystallization and the theory of crystallizers have been ignored completely. Consequently, problems encountered by TVA are not very different from those existing in gypsum processes.

It was the intention of this study to apply the fundamental principles

of crystallization and the theory of MSMPR crystallizers developed by Randolph and Larson to the reaction crystallization of calcium sulfate in a phosphoric acid process. Further it was intended to propose a complete process which would meet most of the objectives laid down before. An additional objective was to undertake investigation on some of the details of the new process and specify the conditions of various operations.

LITERATURE REVIEW

Crystallization Theories

The reaction between calcium fluorapatite and sulfuric acid has been given very little attention from the stand point of crystallization. This reaction crystallization is generally known by the false name of precipitation. Precipitation is an extremely important crystallization process but regrettably it is often not looked upon as such. It has been suggested (25) that those interested in precipitation emphatically should study it as a crystallization phenomenon, particularly paying attention to differential solubility.

Crystallization consists of two processes, nucleation and growth. Exact mechanisms of these processes are not yet fully known. Nucleation is considered to be due to thermodynamically stipulated variations of concentration, called fluctuations (8). These fluctuations consist of complexes of two or more molecules. Some of the fluctuations reach a size possessing the same thermodynamic potential as the surrounding solution. A nucleus is defined (8) as a fluctuation fulfilling this condition. Fluctuations smaller than this critical size possess a predominant tendency to split, while those greater than this size possess a predominant tendency to grow.

Many different theories of growth (6,12,19,34,35) have been proposed. Of these, Volmer's theory (35) based on an adsorbed state has gained considerable ground. His conclusion was that the growth process consists essentially of the continued addition of the repeatable step. Some important general conclusions regarding crystal growth and geometry are

summarized by McCabe (20) as follows:

"1. A crystal that grows under constant external conditions remains very nearly geometrically similar to its original shape but relatively slight changes in conditions may alter the shape.

2. The addition of small amounts of foreign substances may profoundly affect the shape of a growing crystal and its rate of growth.

3. Different faces of the same crystal usually have different translation velocities.

4. Although the exact mechanism and the order of reaction of the growing process are not definitely known, the rate of growth of any particular face in grams per square centimeter is a function of the supersaturation of the bulk of the solution in contact with that face.

5. It is very doubtful that the differences in solubilities of the various faces of a single crystal or of different size particles of the same material, are large enough to influence crystal growth unless the crystals are less than about 2 microns in diameter."

Crystallizer Theories

The practice of industrial crystallization has developed very largely as an art guided until recently (4,27,29,30) by the application of only elementary crystallization theories. McCabe (20) prescribed a number of rules which have become important for industrical crystallization. The development of a suitable theory for crystallizers has been hindered by

the lack of reliable experimental information on nucleation and growth, generally arising due to an inability of the present day techniques to study these molecular processes. McCabe (20) observed that under a variety of conditions the growth rate was proportional to supersaturation and was independent of the crystal size. This observation is referred to as McCabe's ΔL Law, that is each crystal in a suspension will grow the same length in a given time if subjected to the same conditions. However, later work has shown that large deviations from the ΔL Law occur if diffusion controls crystal growth.

In an article by Saeman (30) the theoretical size distribution in a mixed suspension without classified discharge is derived, assuming growth rate as a function of supersaturation only. Bransom et al. (4) treated the theoretical case of a crystallizer of the mixed suspension type. In this work the basic growth rate was assumed to be a function of supersaturation and size of the crystals as well. Saeman (30) and Bransom et al. (4) derived a steady state relationship between population density and particle size for continuous mixed suspension crystallization. This relationship is expressed by the following equation:

$$n_o = n_o^o \exp(-L/r_o T_o)$$

where n_o is the steady state population density, n_o^o the population density of nuclei, L the particle diameter, r the steady state growth rate and T the steady state residence time. It has been shown (21,27,33) that this equation accurately fits data from small experimental as well as large commercial crystallizers.

An extensive theoretical study of unsteady state crystallizers has been carried out by Randolph and Larson (29). They derived important

equations from a crystal numbers balance. Their derivation was based on an arbitrary suspension subjected to the following constraints.

1. The suspension occupies a variable volume V enclosed by fixed boundaries, except for a free gravity surface.
2. This volume has inputs and outputs which can be considered mixed across their respective pipe diameters, but the suspension contained in the volume under consideration is not necessarily mixed.
3. The particles in the suspension are small enough and numerous enough to be considered a continuous distribution over a given volume element of the suspension.
4. No particle breakage occurs, except possibly the chipping of a particle into unequal pieces such that one piece is essentially unchanged in size while the other is small enough to be considered a nuclei.

Using the conservation relationship, accumulation = input-output, they obtained the following numbers balance for particles in an arbitrary size range L_1 to L_2.

$$\frac{d}{dt}\int_V \int_{L_1}^{L_2} \bar{n}\,dL\,dV = \int_{L_1}^{L_2} [Q_i \bar{n}_i - Q_o \bar{n}_o]\,dL \qquad (5)$$

where $\bar{n}$ is the total population density, V is the total suspension volume and $\bar{n}_i$, Q_i and $\bar{n}_o$, Q_o are population density and flow rate of the input and the output streams respectively. By using the rule of Leibnitz on the left hand side of Equation 5 and rearranging they obtained

$$\int_V \left[\frac{\partial \bar{n}}{\partial t} + \frac{\partial}{\partial L}\left(\bar{n}\,\frac{\partial L}{\partial t}\right)\right] dV + \frac{dV}{dt}\,\bar{n}_s - Q_i \bar{n}_i + Q_o \bar{n}_o = 0 \qquad (6)$$

where $\bar{n}_s$ is the local population density of crystals at the suspension surface and is considered constant across the surface. The first term, inside the integral represents the transients in population density of a given size. The second term represents the bulk transport of crystals into and out of the size range due to their growth. The third term represents changes in population due to changes in total suspension volume. The fourth and fifth terms represent inputs and outputs of crystals.

For a continuous, mixed suspension, mixed product removal crystallizer operating under following constraints:

1. constant suspension density
2. no crystal seeding
3. McCabe's ΔL Law holds

Equation 6 reduces to the following form,

$$\frac{\partial \bar{n}}{\partial t} = - r\frac{\partial n}{\partial L} - \frac{n}{T} \qquad (7)$$

where T is the residence time, V/Q. For steady state operation, Equation 7 (subscript o for steady state is deleted for simplicity) reduces to

$$\frac{dn}{dL} = - \frac{n}{rT} \qquad (8)$$

Integrating this,

$$\int_{n_o}^{n} \frac{dn}{n} = - \int_0^L \frac{dL}{rt} \qquad (9)$$

$$n = n^o \exp(-L/rT) \qquad (10)$$

where n^o is the population density of crystals of zero size (nuclei). This equation is identical to Equation 1. Randolph and Larson (29) using a mass balance also showed that under the mentioned constraints, growth rate must be related to the total crystal area in suspension as follows

$$r = -\frac{K_2}{T\int_o^\infty nL^2dL} = \frac{K_2'F}{A} \tag{11}$$

where K_2 and K_2' are proportionality constants, F is production rate and A is total crystal surface area evaluated as

$$A = K_A\int_o^\infty nL^2dL = 2\,K_A\,n^o(rT)^3 \tag{12}$$

where K_A is an area shape factor for the crystals.

Chemical Reactions

The principal reactions (37) in the wet-process phosphoric acid manufacture are as follows:

$$Ca_{10}F_2(PO_4)_6 + 14H_3PO_4 \rightarrow 10Ca(H_2PO_4)_2 + 2HF \tag{13}$$

$$Ca(H_2PO_4)_2 + H_2SO_4 \overset{H_2O}{\rightarrow} CaSO_4\cdot nH_2O + 2H_3PO_4 \tag{14}$$

n = number of water molecules associated with calcium sulfate crystals.

Besides these two reactions, several others take place between phosphate rock impurities and either the phosphoric acid or sulfuric acid. A typical analysis (31) of Florida phosphate rock is given in Table 1. Besides these major constituents, there are present compounds of various other elements (37) in small amounts in the phosphate rock. The ideal

Table 1. Typical analysis of Florida phosphate rock

Component	CaO	P_2O_5	CO_2	F	Fe_2O_3	Al_2O_3	SiO_2
Wt. %	46-50	30-36	1·5-4·4	3·3-4	0·7-2·6	0·7-1·1	7·3-9·8

MgO	SO_3	TOTAL H_2O
0·04-0·5	0·3-1·5	2·6-7·3

rock, from a process standpoint, has a maximum P_2O_5 content and minimum impurities. In addition to reducing the available P_2O_5 content in the rock, impurities can also increase production costs and make the product acid impure (37).

The reaction between CaF_2 of the rock and sulfuric acid is of considerable importance in plant operation.

$$CaF_2 + H_2SO_4 \rightarrow CaSO_4 + 2HF \qquad (15)$$

Hydrogen fluoride that is liberated reacts with silica present in the rock to form fluosilicic acid.

$$6HF + SiO_2 \rightarrow H_2SiF_6 + 2H_2O \qquad (16)$$

The HF and the fluosilicic acid are extremely corrosive compounds and pose a major problem (36) in the wet-process. They may react with sodium or potassium salts present in the rock forming fluosilicates. These fluosilicates have erratic, decreasing solubilities (37) with decreasing temperature, resulting in the formation of a sludge with the $CaSO_4$ in the pipelines, filter cloth and other equipment. This sludge then forms a hard scale requiring plant shut down. When subjected to the acidic

conditions at elevated temperature of the process, some fluosilicic acid decomposes into HF and SiF_4. This silicon fluoride decomposes to gelatinous silica and hydrofluoric acid. The silica then precipitates in the gas ducts and scrubbing system of the plant as a gelatinous solid requiring periodic removal.

Ferric oxide and similar impurities in the rock react with phosphoric acid to form corresponding phosphates. They not only reduce the strength of the product acid but may also come out as heavy sludge when the acid is subsequently concentrated.

Various carbonates present in the rock react with sulfuric acid to form sulfates and carbon dioxide which contributes to foaming problems.

Heat of reactions

The theoretical heat of reaction (37) between tricalcium phosphate, sulfuric acid and water is approximately -80 kg. cal./g. mol. of tricalcium phosphate. The reaction equation is

$$Ca_3(PO_4)_2 + 3H_2SO_4 + 6H_2O = 3CaSO_4 \cdot 2H_2O + 2H_3PO_4 \qquad (17)$$

The total amount of heat released during the wet-process, however, includes this as well as heat of reaction of secondary components in the rock and heat of dilution of phosphoric and sulfuric acids. In most gypsum processes part of this heat has to be removed in order to keep the temperature at a level where only gypsum can precipitate. This requires incorporation of an evaporative cooler in the process.

Phase diagram and solubility data

Calcium sulfate crystallizes in three different crystalline compounds, depending upon the reaction conditions. The phase relationship (37) among

the dihydrate, semihydrate and anhydrite is shown in Figure 1. Because wet phosphoric acid is very impure the transition data vary among different publications. The transition line between semihydrate and anhydrite is the one suggested by Nordengren (23). Higher temperature and acid concentration will induce the formation of the anhydrite. A lower temperature and acid concentration favor semihydrate formation and still lower temperature and acid concentration favor gypsum formation.

The type of calcium sulfate produced and the strength of acid obtained account for the fundamental differences among the several processes that are in use today. Processes involving the formation of gypsum require less severe operating conditions and previously more emphasis has been given to this type of process than any other.

The solubility data for dihydrate and semihydrate (32) are given in Figure 2. It is interesting to note that semihydrate has a higher solubility under some conditions.

The effect of sulfuric acid concentration on the solubility of calcium sulfate (14) is very important in the controlled crystallization of calcium sulfate. This is shown in Figure 3. The solubility is highest when there is no excess sulfuric acid present. The decrease in solubility is very rapid with an increase in sulfuric acid concentration. This would mean that any sudden increase in free sulfate concentration would create a region of very high supersaturation. This condition would result in excessive nucleation. Another effect of higher sulfate concentration is to decrease the solubility of calcium sulfate, resulting in a lower growth rate for the crystals.

Figure 1. Phase diagram of $CaSO_4$ AB: Nordengren's Line (23)
Calculated Line (37)

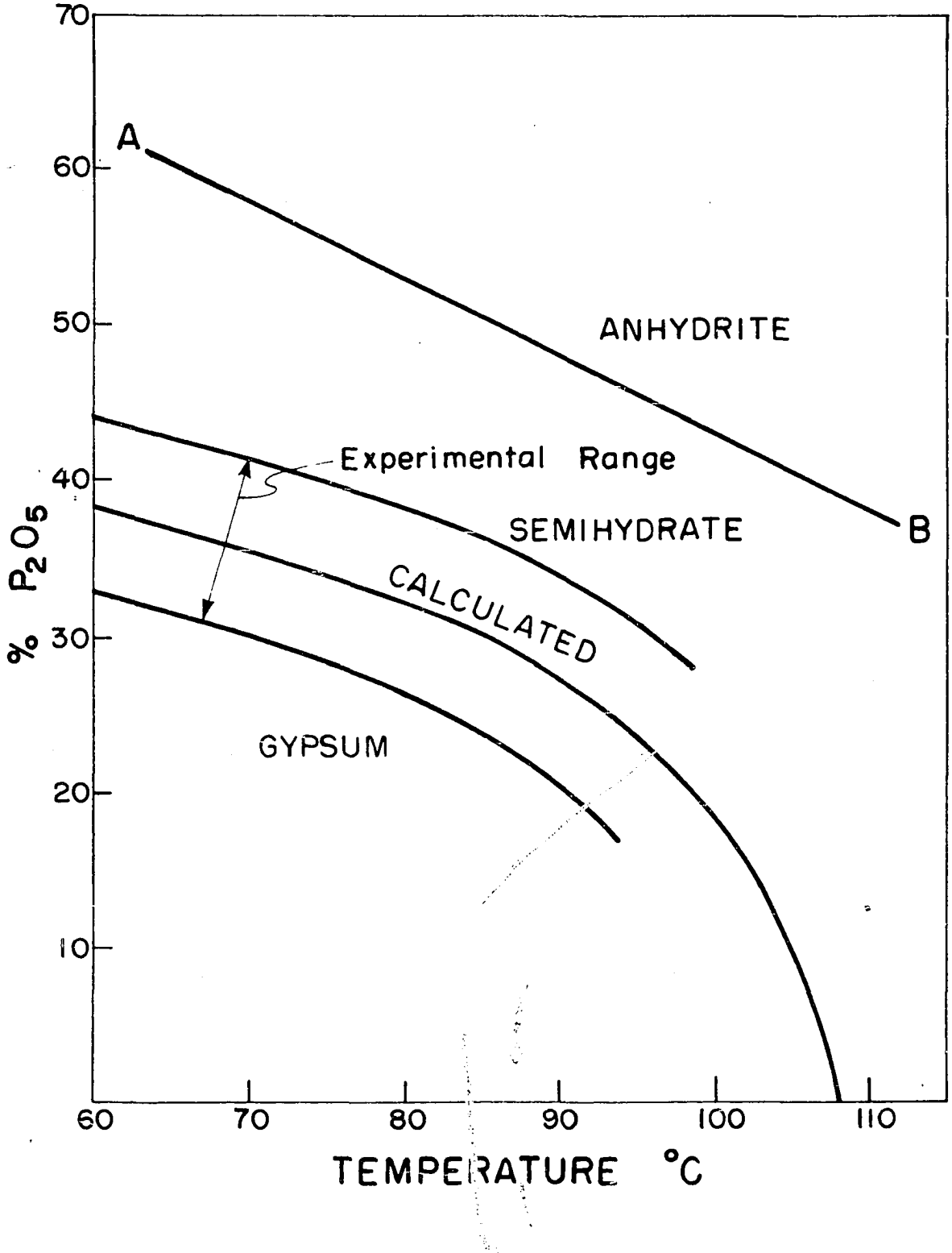
70
60
50
40
30
20
10
% P_2O_5
A
B
ANHYDRITE
Experimental Range
SEMIHYDRATE
CALCULATED
GYPSUM
60
70
80
90
100
110
TEMPERATURE °C

Figure 2. Solubility of calcium sulphate at different temperatures and acid concentrations

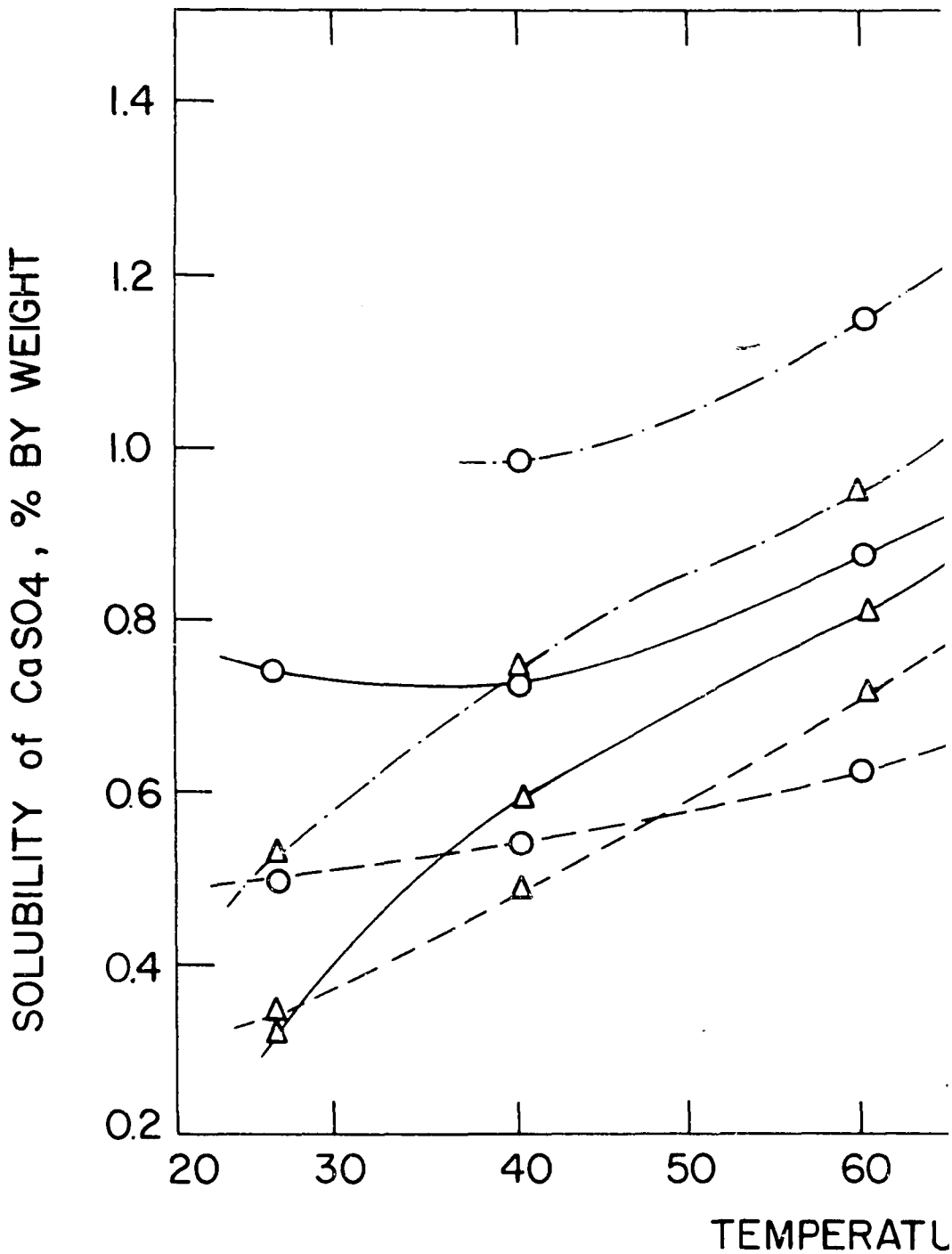
SOLUBILITY of CaSO4, % BY WEIGHT
1.4
1.2
1.0
0.8
0.6
0.4
0.2
20
30
40
50
60
TEMPERATU

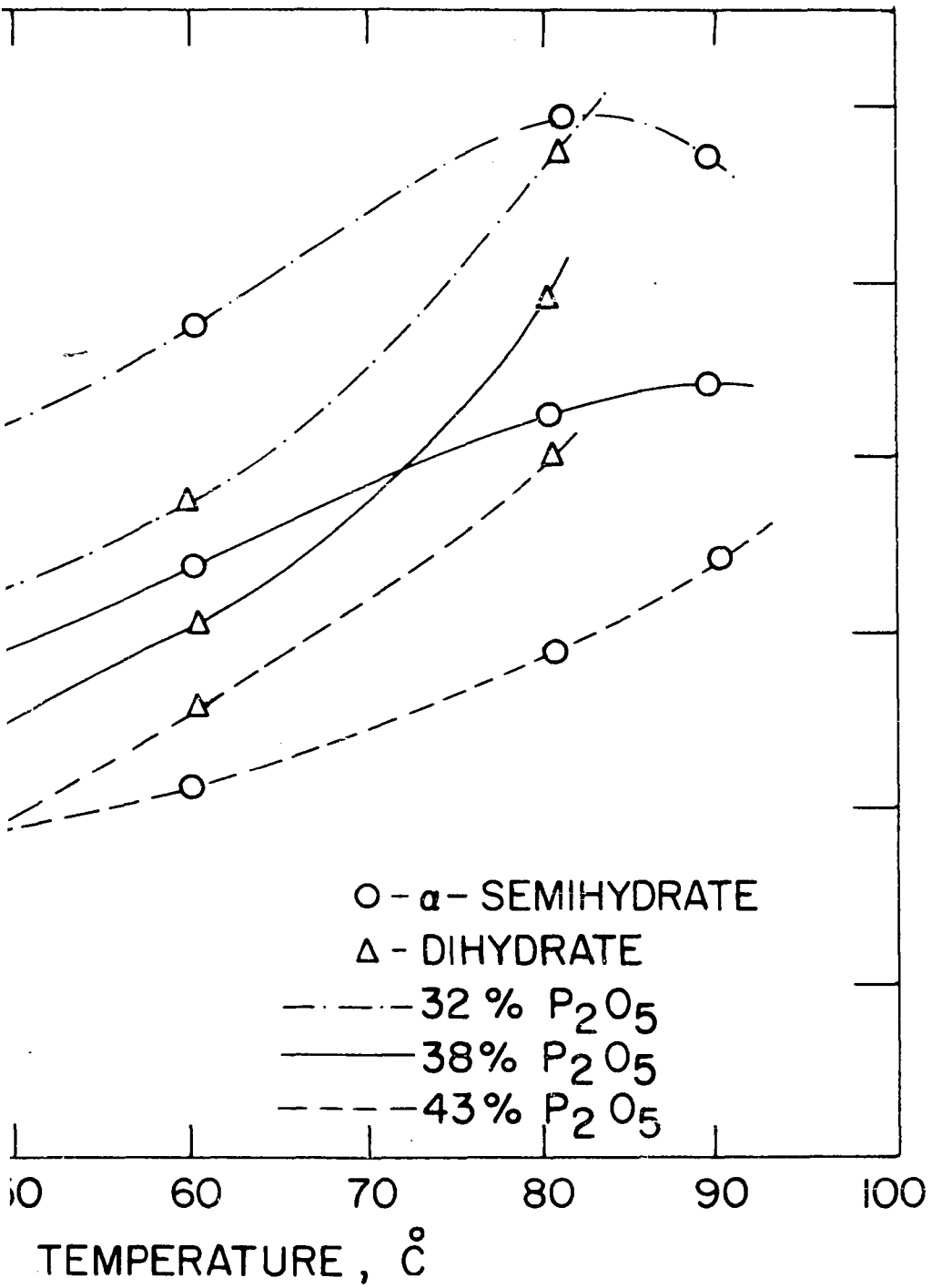
O - α - SEMIHYDRATE
Δ - DIHYDRATE
32 % P_2O_5
38% P_2O_5
43% P_2O_5
60
70
80
90
100
TEMPERATURE, °C

Figure 3. Effect of sulfuric acid concentration on solubility of calcium sulfate in 41.5 percent pure grade phosphoric acid at 70 C°

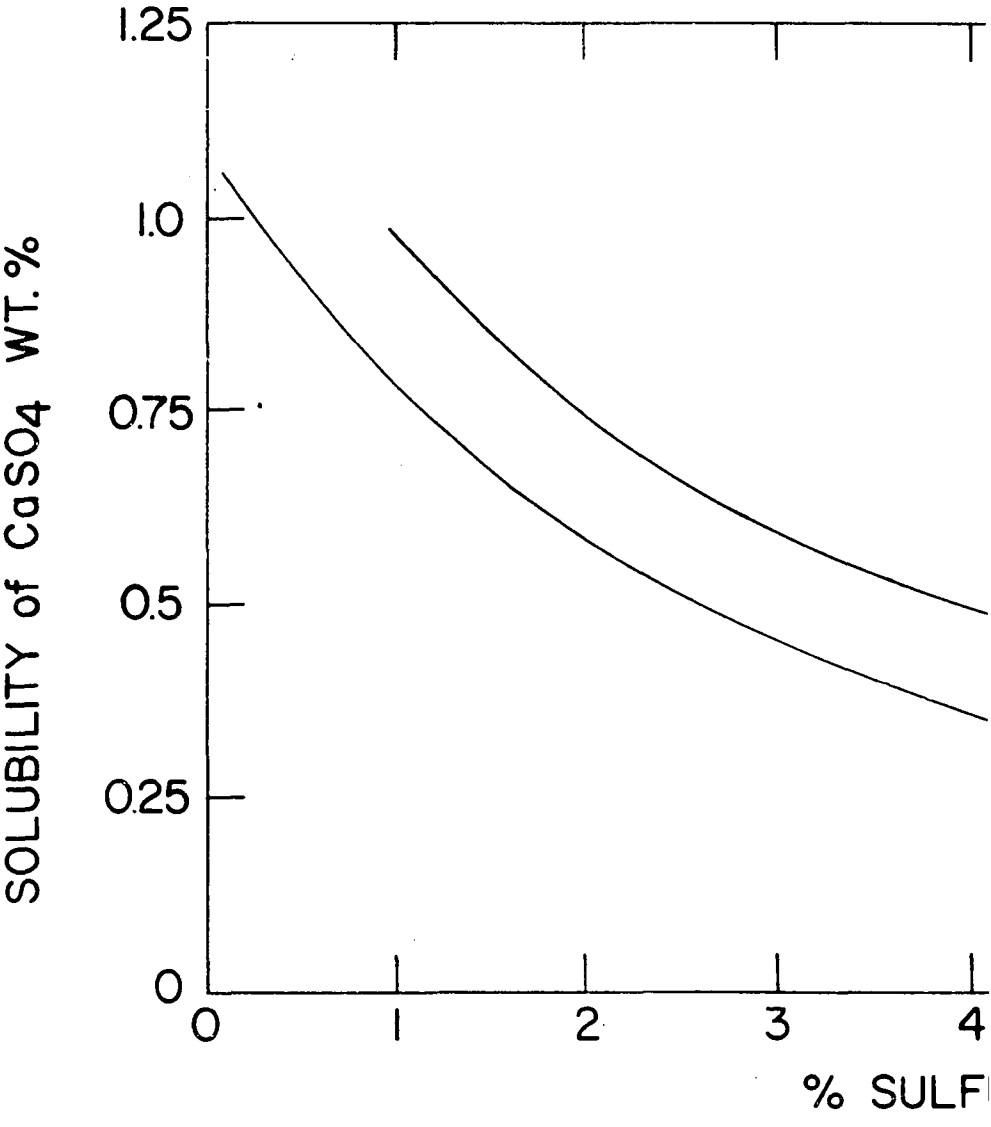
1.25
1.0
0.75
0.5
0.25
0
SOLUBILITY of CaSO4 WT. %
0
1
2
3
4
% SULF

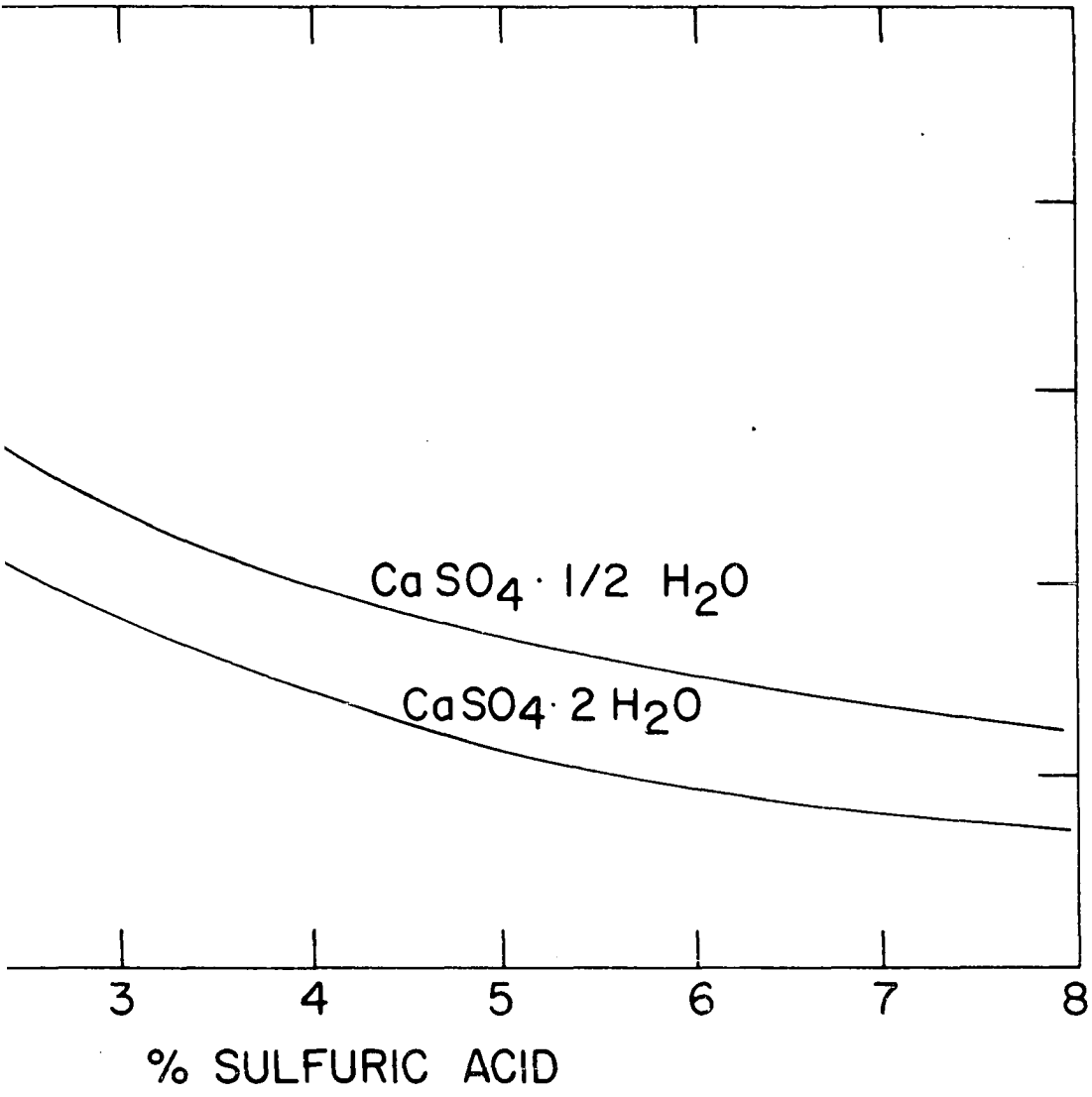
$CaSO_4 \cdot 1/2\ H_2O$
$CaSO_4 \cdot 2\ H_2O$
3
4
5
6
7
8
% SULFURIC ACID

Present Processes

Today most of the wet-process phosphoric acid produced throughout the world is made by the gypsum method. Several different processes (37) are in use today but the difference lies in technology rather than in principle. Following is a list of some of the well known processes:

1. The Dorr-Oliver strong-acid process
2. The Prayon process
3. The Chemico process
4. The Saint Gobian process
5. The Nordengren anhydrite process

The first four processes are based on gypsum crystallization and only the first one will be described here.

The Dorr-Oliver process (37) was developed about 30 years ago and is in world-wide use today. The ground rock flows to a continuously discharging high accuracy weigh scale. The reaction system is in the form of a train of cylindrical tanks with agitators. Agitation requirement in the early stage of reaction is greater; hence more than one small tank is fitted with agitators of high intensity. Strong sulfuric acid is accurately metered and mixed with weak phosphoric acid which is returned from the secondary filtration stage. The combined acids are added to the reaction slurry at a suitable point down stream. This point is quite critical since the location affects both the degree of extraction and the stability of the reaction. Slurry is pumped from one of the last reactors to a vacuum cooler operated under closely controlled conditions so as to maintain a constant reaction temperature. After being cooled, it is returned to the head of the reaction system. Slurry recirculation ratios

may be between 10:1 and 20:1 and are determined by process factors. Slurry, overflowing from the last reactor, is pumped to a traveling-pan filter for separation of the gypsum. Three filtrates, the first is 32% P_2O_5 acid, the second is 18 to 20% of P_2O_5 acid and the third one is the wash liquor of 2 to 5% content, are produced. The strong acid which is the product goes to a concentrator, the weak acid is returned to the reaction system to make mixed acids, and the weak wash liquor is returned to the second filter stage for washing purposes. The gypsum cake is given a final wash with hot water before disposal.

Fumes from the reaction system are removed by a fan and set to a Doyle impingement scrubber. Compounds of silica and fluorine are removed in this scrubber and may be recovered if desired. Over-all recoveries of P_2O_5 in these plants are of the order of 94 to 95 percent.

The Nordengren anhydrite process uses the findings of Nordengren (22). Under controlled circumstances stable crystals of calcium sulfate in an anhydrous or partly hydrated form result. These can be readily filtered and purified by washing with water. Several methods of dissolving phosphate rock to produce phosphoric acid and anhydrite crystals were initiated, but major factors, extreme corrosion and process control, presented the difficulties. A few small plants based on this process are in operation in Europe. These plants produce an acid containing 40 to 45% P_2O_5. A temperature of 135°C is maintained in the reaction vessel.

A novel method incorporating solvent extraction has recently (11) been described. Many groups are now working on this process. In the process phosphate rock is digested with by-product hydrochloric acid and the slurry is extracted with an organic compound. The economics of the

process (24) however, are said to be posing problems. The process may compete with the electric furnace method but the acid produced is too expensive to compete with the fertilizer grade acid. The cost of P_2O_5 as electric-furnace acid is nearly twice the cost of the wet-process material.

THEORETICAL CONSIDERATIONS

Crystallization Principles and Phosphoric Acid Process

Any new wet-phosphoric acid process must be designed with due regard to contemporary theories of crystallization and crystallizer design. Thus it is necessary to outline the general basic principles of the process and to identify the conditions under which the crystallization must take place. The principal reactions are

$$Ca_{10}F_2(PO_4)_6 + 14H_3PO_4 \rightarrow 10Ca(H_2PO_4)_2 + 2HF \quad (18)$$

and

$$Ca(H_2PO_4)_2 + H_2SO_4 \rightarrow CaSO_4 + 2H_3PO_4 \quad (19)$$

It can be seen that the second reaction creates the supersaturation of $CaSO_4$ in the liquid phase. For an efficient phosphoric acid process, this supersaturation must be controlled.

The first reaction occurs between solid rock phosphate and liquid phosphoric acid. The main product, monocalcium phosphate, dissolves in phosphoric acid and then reacts with sulfuric acid. The complicated chemical structure of phosphate rock, impurities and particle size make this reaction very difficult to carry out rapidly and completely. The chemical composition of phosphate rock, even from the same source, varies considerably. Impurities in the rock constitute the side reactions and consume acid. In such a complex situation, when this second reaction is carried out simultaneously in the same reactor, a relatively uncontrollable crystallization process results. Monocalcium phosphate, formed on the surface of the rock particles by the first reaction, reacts further with sulfuric acid forming a hard coating of $CaSO_4$ on the rock particles. This

unreacted phosphate rock in the center of the particle is trapped without allowing further reaction. This unreacted rock phosphate constitutes a serious loss of raw material in the commercial processes where these reactions are crried out simultaneously.

Good control of the crystallizer can only be obtained if feed rates of the reactants are in proper stoichiometric ratios. Feeding of solid phosphate rock, with its constantly varying complex composition, in proper stoichiometric ratio to sulfuric acid feed rate is an almost impossible task. Moreover, an unpredictable amount of phosphate rock would remain unreacted, depending upon its physical characteristics. Under some conditions dicalcium phosphate, $CaHPO_4$, is formed instead of monocalcium phosphate. Gypsum and dicalcium phosphate have almost identical crystal structure and molecular weight and may form a solid solution upon crystallizing. This not only constitutes a loss of P_2O_5 but creates an imbalance in the reactant ratio as well.

It is obvious then, that in order to achieve good control over the reaction crystallization, the above two reactions should be carried out in separate reactors. The second reaction, which results in crystallization of $CaSO_4$, would then become the central step in a new phosphoric acid process. The product of the first reaction consists chiefly of monocalcium phosphate. The impurities are carried with it from the phosphate rock. This product can be dissolved in phosphoric acid to obtain a solution of monocalcium phosphate. If desired, the insoluble impurities, like silica and organic matter, can be filtered off. Then the second reaction involving crystallization of $CaSO_4$ can be carried out fully, meeting the requirements for complete control of the

supersaturation.

Kinetics of Calcium Sulfate Crystallization

At constant suspension density the steady state mathematical model of a MSMPR crystallizer, developed by Randolph and Larson (29), can be used to determine the kinetics for calcium sulphate crystallization. It is assumed in the treatment that the kinetics of nucleation and growth can be represented as simple power functions of supersaturation as follows.

$$\frac{dN^o}{dt} = K_n S^a \tag{20}$$

and

$$r = K_g S^b \tag{21}$$

where N^o is the number of nuclei, S the supersaturation, r the growth rate, K_n and K_g are proportionality constants, and a and b are constants which are to be determined. Since $r = \frac{dL}{dt}$ and $n = \frac{dN}{dL}$ the nucleation rate can be written as:

$$\frac{dN^o}{dt} = \frac{dL}{dt}\left(\frac{dN}{dL}\right) L = 0 = rn^o \tag{22}$$

By combining Equations 20, 21 and 22, and by eliminating S and dN^o/dt, the following relationship between nuclei population density and growth rate for the calcium sulfate system is obtained.

$$n^o = K_1[r]^{(a/b\ -1)} \tag{23}$$

where K_1 is a proportionality constant. This equation indicates that a plot of log n^o versus log r should be a straight line with the slope of (a/b -1). Equation 23 can be used to find (a/b -1) experimentally by conducting a series of steady state experiments at different residence

times (i.e., different growth rates). An analysis of the steady state crystal distribution for each residence time can be plotted as L versus log n. These plots present a method for determining n^o and r. The intercept is numerically equal to n^o and the growth rate is inversely proportional to the slope of the resulting straight line. A plot of log n^o versus log r can now be made. The intercept and slope give the values of K_1 and (a/b -1) respectively. The number (a/b -1) is called the kinetic order of the system and is the essential parameter for determining the size distribution of the crystal product.

Suspension Density

Suspension density, defined as the weight of crystals per unit volume of crystal mother liquor slurry is an important variable in industrial crystallizers. Supersaturation may be a function of the suspension density and therefore nucleation and growth rates may be affected by changes in this parameter. Another important effect, as suggested by a number of investigators (26,27) is the effect that suspended solids may have on the basic nucleation mechanisum. The existence of two fundamental nucleation processes, homogenous and heterogeneous, is well-known. In the former case the nucleation process is solely due to supersaturation while in the later case it is also dependent upon the solids that are held in the suspension. A number of authors have given various explanations for the effect of solids in suspension on nucleation. Among these are fracture of dendritic growth, the sweeping away from the neighborhood of the individual crystals a reservoir layer of high solute concentration (3), attrition, and catalysis.

Larson et al. (16) have made a theoretical analysis of a MSMPR crystallizer for the following two cases, (i) when nucleation rate is independent of suspension density, and (ii) when nucleation rate is dependent on suspension density.

In order to determine if the nucleation mechanism for calcium sulphate is a homogenous process or a heterogeneous process it would be necessary to investigate the mathematicl models of MSMPR crystallizer for the above two cases. Analyses of the data obtained from known variations in suspension density in a MSMPR crystallizer, using these models, can reveal the nature of nucleation process.

Nucleation rate - independent of suspension density

In this case the nucleation rate equation is the same as Equation 20 which is

$$\frac{dN^o}{dt} = K_n S^a$$

and for $r = \frac{dL}{dt} = K_g S^b$ Equation 20 can be written as

$$\frac{dN^o}{dt} = K_1 r^{a/b} \tag{24}$$

Using Equation 22 therefore,

$$n^o = K_1 [r]^{(a/b\ -1)} \tag{25}$$

For two steady state MSMPR crystallizers operating under the same conditions but with different suspension densities, Equation 11 can be used to write the following expression,

$$\frac{r_1}{r_2} = \frac{\int_0^\infty n_2 L^2 \, dL}{\int_0^\infty n_1 L^2 \, dL} \times \frac{F_1}{F_2} \tag{26}$$

Substituting Equation 10 and integrating,

$$\frac{r_1}{r_2} = \frac{n_2^o}{n_1^o} \times \frac{r_2^3}{r_1^3} \times \frac{F_1}{F_2} \tag{27}$$

But F , the production rate, is proportional to suspension density ϕ in the crystallizer and

$$n^o = K_1 [r]^{(a/b - 1)}$$

therefore,

$$\frac{r_1^4}{r_2^4} = \left(\frac{r_2}{r_1}\right)^{(a/b - 1)} \cdot \frac{\phi_1}{\phi_2} \tag{28}$$

or

$$\left(\frac{r_1}{r_2}\right)^{(3 + a/b)} = \frac{\phi_1}{\phi_2} \tag{29}$$

Equation 29 can be used to test the data obtained by variation of suspension density for homogeneous nucleation. Another relationship, which can be used to check the data for homogeneous nucleation, can be derived from Equation 25. For two levels of suspension density,

$$\left(\frac{n_1^o}{n_2^o}\right) = \left(\frac{r_1}{r_2}\right)^{(a/b - 1)} \tag{30}$$

Nucleation rate - dependent on suspension density

For a crystallization system in which nucleation rate depends on solids concentration in suspension, a mathematical model incorporating a suspension density dependent nucleation rate must be used. Therefore,

$$\frac{dN^o}{dt} = K_n \phi^d S^a \tag{31}$$

Using $r = K_g S^b$ Equation 31 can be written as

$$\frac{dN^o}{dt} = K \phi^d r^{a/b} \tag{32}$$

and since

$$\frac{dN^o}{dt} = r\, n^o$$

it follows that

$$n^o = K \phi^d r^{(a/b - 1)} \tag{33}$$

Proceeding further as in the previous case the following relationships are obtained.

$$(\frac{r_1}{r_2})^4 = \frac{F_1}{F_2} \cdot (\frac{\phi_2}{\phi_1})^d \cdot (\frac{r_2}{r_1})^{a/b - 1} \tag{34}$$

For the case when d = 1 and since $F_1/F_2 = \phi_1/\phi_2$

$$(\frac{r_1}{r_2})^{a/b + 3} = 1 \tag{35}$$

and

$$\frac{n_1^o}{n_2^o} = \frac{\phi_1}{\phi_2} \tag{36}$$

which implies that if nucleation rate is linearly dependent on suspension

density the growth rate will not change with suspension density and nucleation will increase directly in proportion to the increase in suspension density. For the case when $d \neq 1$, the growth rate and nucleation rate will be affected in a nonlinear manner for variation in suspension density.

Crystal Habit

Gypsum crystals are known to have various habits. Impurities present in phosphate rock have been shown to affect (9) the crystal habit of gypsum produced in the phosphoric acid manufacture. It is desirable to have calcium sulphate crystals which are large and symmetric in shape. Long needles, thin plates of agglomerated spherulite crystals are very difficult to filter and wash.

Present views on the habit of gypsum crystals are confusing and contrasting (9,37). Weber and Pratt (37) emphasize that the sulphate concentration of the slurry liquor is the prime cause of various habits of gypsum. Larson and Larson (15) have investigated the effect of several impurities on size distribution of gypsum crystals obtained by reaction crystallization in a batch crystallizer using monocalcium phosphate and sulfuric acid feeds.

Close control of sulfate ion concentration in the wet-process has been emphasized as being very important for proper crystallization and filtrability of gypsum. Its control has always been difficult because of inadequate control equipment for feeding solids. Moreover the composition of phosphate rock, to a certain degree, is continuously changing. This results in poor control of excess sulfuric acid that is required in

the process slurry. An excess of 1 to 2 percent sulfuric acid is required in order to reduce the loss of P_2O_5 due to co-crystallization of $CaHPO_4 \cdot 2H_2O$ and gypsum. Crystal structures of these two compounds are very similar and they are known to form a solid solution (12).

The importance of close control of excess sulfate ion concentration can be due to two reasons. The first one is due to its effect on the solubility of calcium sulphate in the process slurry. Figure 3 shows the effect sulfuric acid concentration has on the solubility of gypsum (12a) in the mixed acids. Solubility of already sparingly soluble calcium sulphate decreases sharply with a slight increase in the sulfuric acid concentration. This would mean that in the reaction zones where excess sulfuric acid concentration fluctuates, the changes in supersaturation are of considerable magnitude. This is exactly the condition which causes excessive nucleation.

The second reason is that an excess of sulfate ions in the process slurry cause an impervious layer of calcium sulfate to be formed on the surface of each rock particle, thus preventing further digestion. This leads to an increase in the extraction loss.

There is no theoretical explanation available which shows why proper control of sulfate concentration is important for crystallization of large, symmetric gypsum crystals. An attempt is made here to explain this phenomenon with the help of the atomic structure of the gypsum crystal (2,7,15). The structure is of a layer-lattice type with water molecules between sheets composed of chains of alternate Ca^{++} and SO_4^{--} ions. The chains are arranged to give a corrugation effect within the sheets. Figure 4 shows one such sheet. The distance between the sheets

Figure 4. Atomic structure of $CaSO_4 \cdot 2H_2O$ lattice plane

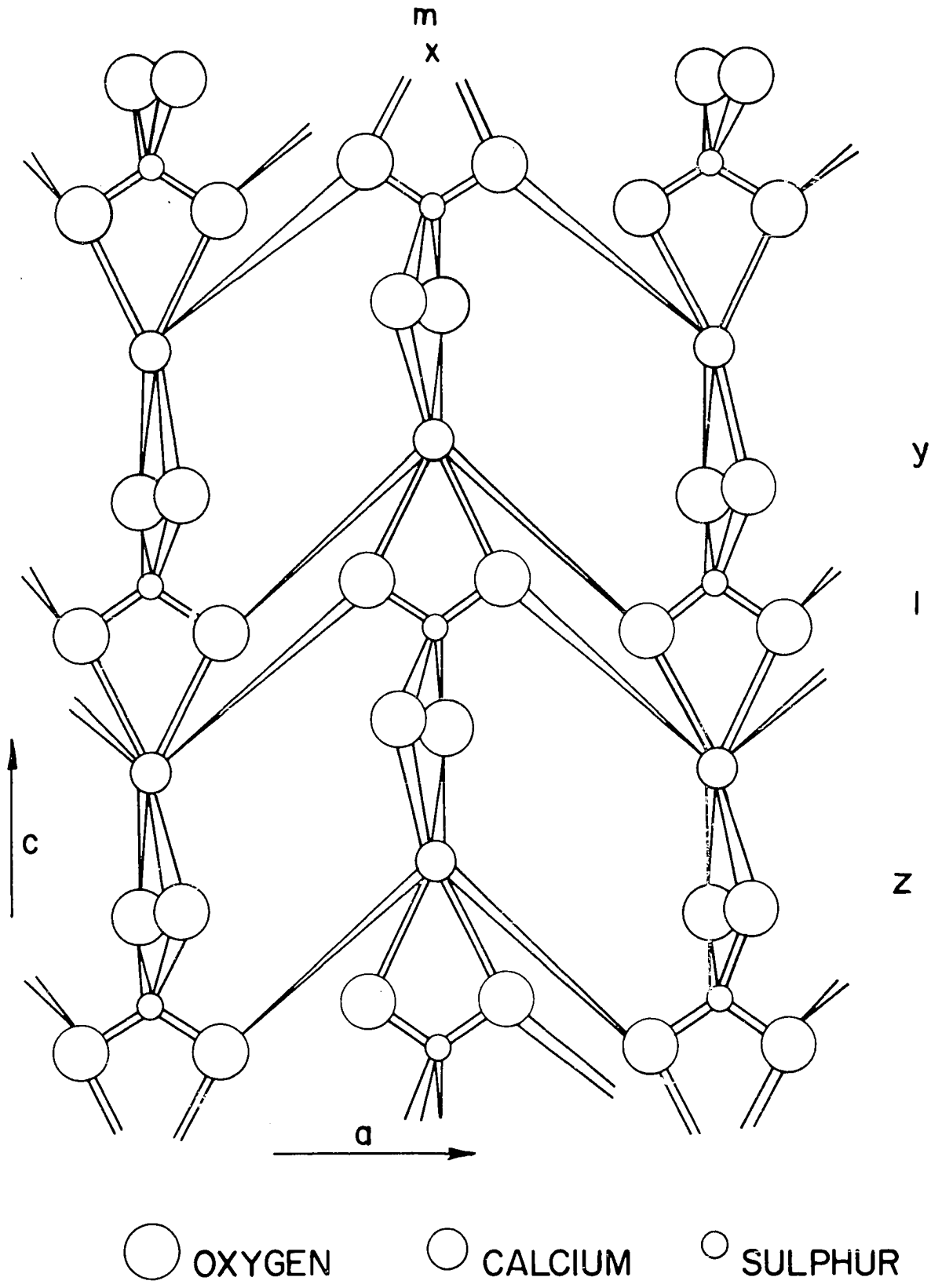
m
x
y
l
z
c
a
OXYGEN
CALCIUM
SULPHUR

is equal to b/2 = 7·585 A. The unit cell dimensions are a = 5·70 A, b = 15·17 A, c = 6·502 A and β = 118° 23'.

Now suppose that the sheet in Figure 4 is the top sheet on the surface of a gypsum crystal growing in the slurry. In order for the crystal to grow it must obtain Ca^{++}, SO_4^{--} and H_2O from its surroundings. If a calcium ion associates itself with the position x, the free energy change that is involved will be more than if it were to associate itself with positions at either y or z. Once a calcium ion rests at x, the free energy change for associating a SO_4^{--} at m, next to x, along the same chain will be more than that associated with its locating at the position 1. Now, the positioning of calcium ions along the other two chains in the c direction and on either side of m will be more likely, since they each involve the use of three free valencies. Similarly, association of a calcium ion at position y is more probable than at a position on top of the sheet in the direction of the b axes. Successive sheets in the b direction are connected by water molecules and the related bond strength is the weakest, so the free energy change involved will be a minimum in this direction. Since the growth rate is the fastest in the direction where free energy change is the highest, one would expect the fastest growth rate of the gypsum crystal along the c axis, the lowest growth rate in the direction of the b axis, and with an intermediate growth rate in the direction of the a axis.

Growth is also dependent on the diffusion of the different ions and water molecules that are involved. Diffusion of SO_4^{--} will be the slowest because of its large volume and weight when compared to the rates of diffusion of calcium ions and water molecules. High viscosity and density

of surrounding phosphoric acid and the sparing solubility of gypsum would indicate that the growth rate is diffusion controlled. Increased availability of SO_4^{--} ions, therefore, would result in a rapid growth of crystal in the c axis direction. This condition of increased availability of SO_4^{--} ions is obtained either at high supersaturation or when there is an excess of free sulfuric acid present in the slurry. It can be concluded therefore, that decreasing the SO_4^{--} ions concentration or in other words increasing the Ca^{++} ions concentration would tend to reduce the length of needle like crystals.

Now consider a thin long needle-like crystal in the slurry, surrounded by a liquid film through which diffusion of calcium sulfate takes place. Obviously, the thickness of this film will be different on different surfaces. The thickness of the film on the two ends of the needle would be expected to be the least considering its shape and its motion in the liquid. Of more importance is the fact that this film is continuously being pierced by the crystal because of its growth on the ends. This brings the end surfaces into the fresh regions of supersaturation continuously for further growth.

The structure of the semihydrate form of calcium sulphate is not yet properly defined in the literature. However, Caspari (7) and Bunn (5) suggested that the structure was essentially a framework of Ca^{++} and SO_4^{--} ions, penetrated by channels capable of accomodating the water molecules. If this is true, then the structure of semihydrate can be considered to be similar to the gypsum crystal structure which is made up of chains of Ca^{++} and SO_4^{--} ions. Both have monoclinic configurations in common. In this case the effect of Ca^{++} concentration will probably be the same for

both crystal structures.

Growth Rates and Crystal Forms

The relative magnitude of growth rates for the three different forms of calcium sulphate can be discussed from a thermodynamic point of view. Calcium sulphate anhydrite crystals would probably grow at a faster rate than semihydrate or dihydrate because only Ca^{++} and SO_4^{--} ions need be transported for its growth; while in the case of semihydrate, an additional half molecule of water, and in the case of dihydrate, two molecules of water, have to be transported to the growing crystal surface per molecule of $CaSO_4$. Since dilution of phosphoric acid by water is an exothermic process, removal of water from the acid by crystallization would be an endothermic process. Of course, when the water molecules reach their positions on the crystal surface, the process of crystallization would be exothermic to a small extent, since crystal bonds are formed. Thus the semihydrate crystallization process requires less mass and heat transfer than gypsum, which should result in a more rapid crystal growth for it.

EXPERIMENTAL WORK AND RESULTS

Equipment and Procedures

A continuous mixed suspension, mixed product removal crystallizer was built to carry out all the crystallization work. A schematic diagram of the complete arrangement is shown in Figure 5.

The crystallizer consisted of a round bottom glass vessel, equipped with an agitator and baffles, and was submerged in a constant temperature bath. The normal operating capacity of the crystallizer was one liter. This design allowed the simulation of perfect mixing conditions. Feeds were introduced to the crystallizer through a diaphragm type Mec-O-Matic metering pumps. Metering the corrosive, scale forming acid was found extremely difficult. Check ball valves made of glass were attacked by impure phosphoric acid which contained fluorine compounds. Scale formation was also a problem for maintaining constant feed rates. Continuous withdrawal of mixed suspension from the crystallizer was achieved by the introduction of an overhead glass tube which was connected to a vacuum as shown in Figure 5. This arrangement maintained a constant volume in the crystallizer and also permitted changes to be made in the volume of the crystallizer whenever desired. High viscosity of the slurry and fineness of the crystals prevented settling problems.

Feed solutions were prepared from the reagent grade monocalcium phosphate monohydrate and sulfuric acid of proper concentration. Crystallization data were also obtained using commercial grade chemicals, thus simulating the conditions that would exist in a process to be proposed. For this purpose, commercial triple super-phosphate was dissolved in

Figure 5. Schematic diagram of the continuous crystallization apparatus

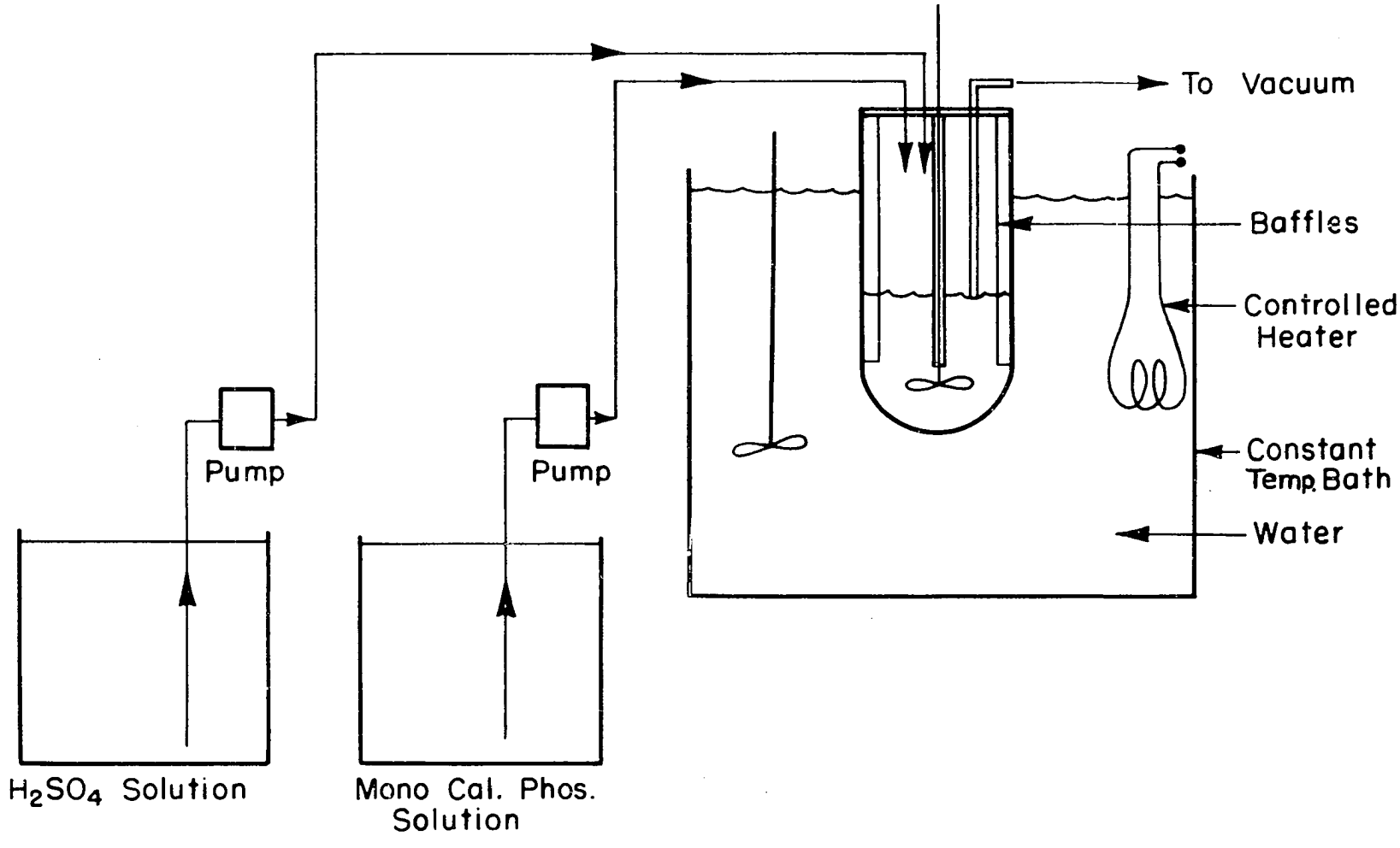
To Vacuum
Baffles
Controlled Heater
Constant Temp. Bath
Water
Pump
Pump
H_2SO_4 Solution
Mono Cal. Phos. Solution

diluted commercial wet-process phosphoric acid. The solution was filtered to remove silica and other solid impurities. Similarly, sulfuric acid feed solution was prepared by mixing sulfuric acid with diluted wet-process acid.

Several preliminary runs were carried out with a MSMPR crystallizer, subjected to various operating conditions, to determine suitable ranges. At temperatures lower than 60 C° and acid concentration less than 30% P_2O_5, $CaSO_4$ crystallized as gypsum. At temperatures above 70 C° and acid concentrations above 40% P_2O_5, semihydrate was crystallized. A marked difference in their growth rates was observed. Semihydrate crystals of comparatively large size were obtained in a relatively short period. Cypsum crystals, for the same residence time, were found to crystallize in a needle habit of extremely small size. This habit was very unfavorable for filtering, washing and sizing on the Coulter Counter. During counting, they immediately blocked the aperture and thus their size distribution was impossible to obtain by the Coulter Counter. As compared to this, semihydrate crystals of hexagonal prismatic habit were found to be easy to filter, wash and analyze on the Coulter Counter.

Another problem with gypsum crystallization was due to changes in the phosphoric acid concentration within the crystallizer. Comparatively long draw down times were required to obtain gypsum crystals of reasonable size which could be filtered, washed and counted on the Coulter Counter. Because of this long residence time, relatively dilute phosphoric acid became more concentrated due to evaporation. This changed the form of the calcium sulfate crystals from gypsum to semihydrate.

These problems with gypsum crystallization restricted the

experimental work mainly to semihydrate form of calcium sulfate. Advantages of a process based on semihydrate crystallization have already been discussed. Preliminary experimental work thus established a more favorable habit and nucleation and growth kinetics for the semihydrate form.

All the MSMPR runs were carried out at steady state. The acid concentration in the suspension was 42 percent P_2O_5, except where noted otherwise. During each run the feed rates, the temperature and the volume of the suspension were maintained constant. At least 12 draw down times (residence times) were allowed to elapse before sampling of the steady state crystal suspension. It was found that this amount of time was necessary for the suspension to approach the steady state operating condition. This was confirmed by size distribution analyses.

Sampling of the crystal suspension was carried out by the use of an evacuated cylinder. This procedure permitted very fast sampling and eliminated possibilities of classification during sampling. Here again the fineness of crystals and the high viscosity of the slurry were favorable factors for mixed product removal. The slurry sample was weighed and filtered immediately under vacuum. Crystals were washed with 10 milliliters of water at 55 C°, immediately washed with absolute alcohol and dried in an oven at 65 C°. The crystals were weighed and sealed in a sample bottle. Percent suspension density was calculated as the weight of the crystals in grams per 100 grams of the slurry.

Size analyses of the steady state sample was obtained using the Coulter Counter. This electronic instrument was used to determine the

number and size of particles suspended in an electrically conductive liquid. To accomplish the analyses, the suspension flows through a small aperture having an immersed electrode on either side. Crystal concentration must be such that the crystals traverse the aperture substantially one at a time. Each particle on passage displaces electrolyte within the aperture, momentarily changing the resistance between the electrodes, thus producing a voltage pulse of a magnitude proportional to particle volume. The resultant series of pulses are electronically amplified, scaled and counted. Pulses are also fed to a series of threshold circuits having adjustable screen-out voltage levels. This apparatus was an excellent device to find the size distribution of calcium sulfate crystals, which were too small to analyse by other conventional methods.

Experimentally, a sample of crystals was weighed and slurried in 220 milliliter of electrolyte, 4% ammonium thiocyanate dissolved in isopropyl alcohol. Two milliliter of this mixed suspension was drawn through the aperture and all crystals that were larger than those corresponding to the threshold setting were counted. By repeated counts at various thresholds, data were obtained that allowed the calculation of the size distribution of particles in the slurried mixture. The counting of the smaller sizes of crystals was limited by the cross-sectional area of the aperture selected and the shape of the crystals. Needle like, long crystals would normally block the aperture if the size of the aperture was smaller than the length of the needles. Another physical limitation was the counting of very few large crystals. In order to get correct count of these crystals, it was necessary to have to repeat the counting procedure of each threshold setting for several times. However, repeating the

results for the large particles was not possible because the amount of slurried electrolyte that can be used with the Coulter Counter Model A was limited. Thus the accuracy of the size distribution for the larger sized crystals is less than that for the smaller crystals.

Population density values for different sizes were calculated by the approximation, $n = \frac{\Delta N}{\Delta L}$, from the size distribution data, numbers versus size. The basis for the population density can be arbitrarily chosen depending upon its use. In most cases, it was based on 9.1×10^{-5} grams of crystals unless indicated otherwise. A plot of log n versus L was made for each steady state run. From the slope and intercept, growth rate r and nuclei population density n^{o} were obtained.

Analyses of crystal samples for total P_2O_5 was carried out by the official method of the Association of Official Agricultural Chemists (1). Water of crystallization was determined after prolonged heating of the samples at 250 C°.

Temperature

Seven steady state runs, shown in Table 2, four using impure feeds and three using pure feeds, were carried out to investigate the effect of temperature. Temperature was varied from 45 C° to 76 C°. Growth rates and nuclei population densities were obtained from the steady state runs. The data obtained are summarized in Figure 6. An increase in temperature increases the growth rate considerably, however, this increase tapers off above 65 C°, for the impure system. Variations in temperature also affect the crystalline water content, as shown in the Figure 6. Water content of crystals obtained from impure feeds increases from 7.78% to 13-14% as

Figure 6. Effect of temperature on growth rate and nuclei population density of semihydrate crystals in pure and impure phosphoric acid. Numbers in rectangles represent corresponding percent crystalline water content

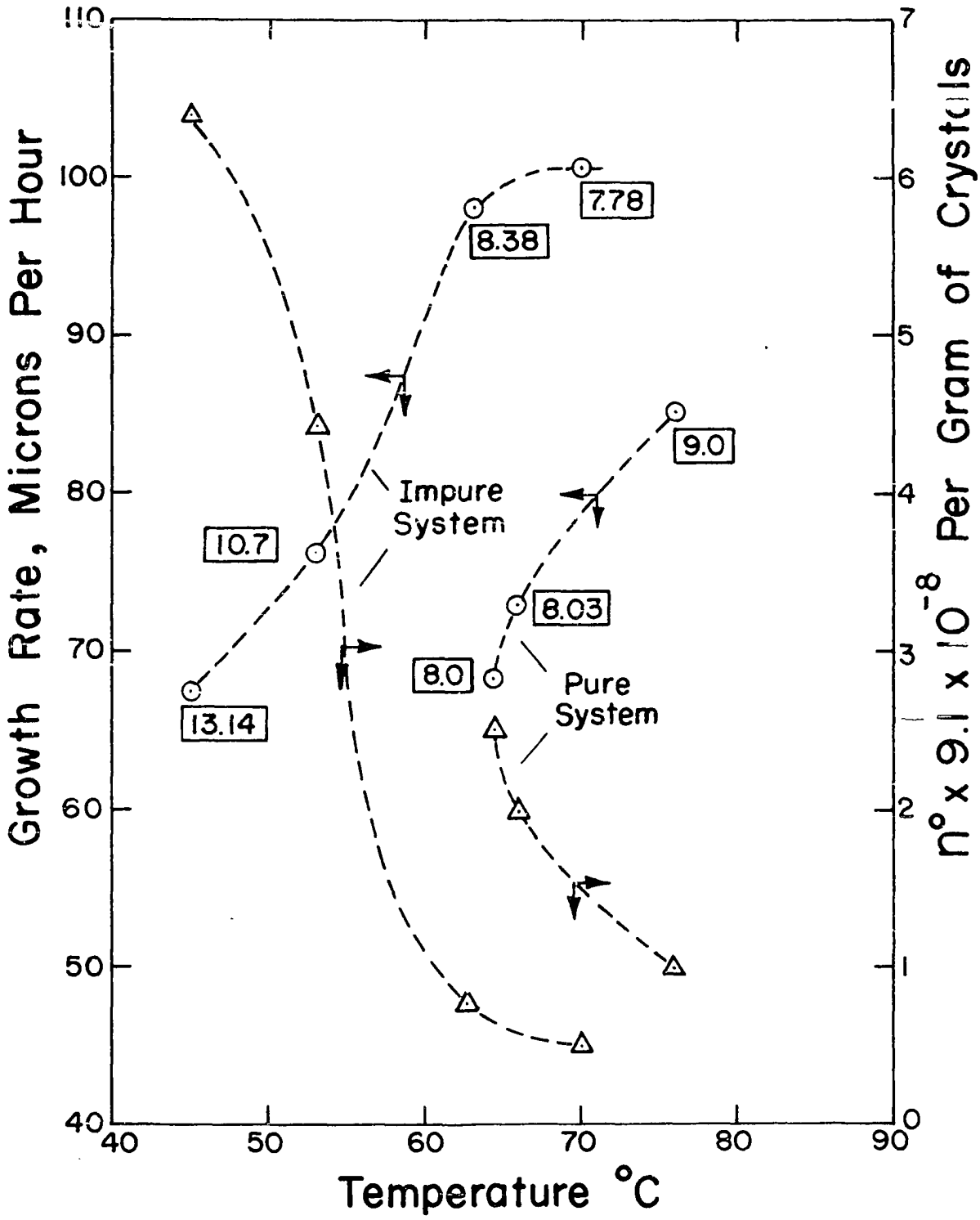
Growth Rate, Microns Per Hour
n° x 9.1 x 10⁻⁸ Per Gram of Crystals
Temperature °C
110
100
90
80
70
60
50
40
7
6
5
4
3
2
1
0
40
50
60
70
80
90
7.78
8.38
9.0
10.7
8.03
8.0
13.14
Impure System
Pure System

Table 2. Variation of temperature

Run No.	Temp C°	% suspension density	Residence time T minutes	Growth rate r microns per hour	% water of crystallization
			PURE ACID		
31	70	0.650	37.5	100.5	7.78
32	63	0.641	37.5	97.7	8.38
33	53	0.640	37.5	76.0	10.70
34	45	0.643	37.5	67.4	13.14
			IMPURE ACID		
35	76.0	3.763	38.3	84.9	9.00
36	64.5	3.610	38.3	68.3	8.00
37	66.5	3.870	38.3	72.8	8.03

temperature is decreased from 70 C° to 45 C°. This indicates partial transformation of semihydrate crystals into dihydrate. Stoichiometric water content of semihydrate and dihydrate crystals is 6.21 and 20.9 percent respectively. However, crystalline water content of semihydrate has been found to vary between 6.21 % ($\frac{1}{2}$ H_2O) and 8.1 % ($\frac{2}{3}$ H_2O) by many researchers (2,5).

Important conclusions can be derived from the results obtained. Crystallization of calcium sulphate as semihydrate is much more favorable than as gypsum because of the significant advantage of much higher growth rate that can be obtained. Higher temperatures are favorable for increasing the growth rate. A six fold decrease in the population density of nuclei is achieved by increasing temperature from 45 C° to 70 C°.

Nucleation rates for each of the steady state runs can be calculated using the equation

$$\frac{dN}{dt} = n^{o}\ r$$

A plot of nucleation rate versus temperature is presented in Figure 7.

At lower temperatures, the gypsum crystal habit dominates, thus making an analyses of these extremely small, needle like crystals very difficult with the Coulter Counter.

Phosphoric Acid Concentration

Phosphoric acid concentration in the crystallizer was varied, using pure grade feeds, in three different steady state runs shown in Table 3, with all other conditions unchanged in an effort to determine the effect of acid concentration on crystallization kinetics. Steady state plots,

Table 3. Variation of acid concentration

Run No.	Temp C°	% suspension density	Residence time T minutes	% H_3PO_4	Growth rate r microns per hour
49	72.5	4.04	65	49.5	40.3
50	70.5	4.05	65	53.8	41.5
51	73.0	4.00	65	58.0	40.5

Figures 8, 9, and 10 were made to find growth rates and nuclei population densities. Phosphoric acid concentration was varied from 49.5% to 58%. From the results, it was found that phosphoric acid concentration has almost no effect on growth and nucleation in the range investigated.

Figure 7. Plot of nucleation rate versus temperature for pure and impure feeds

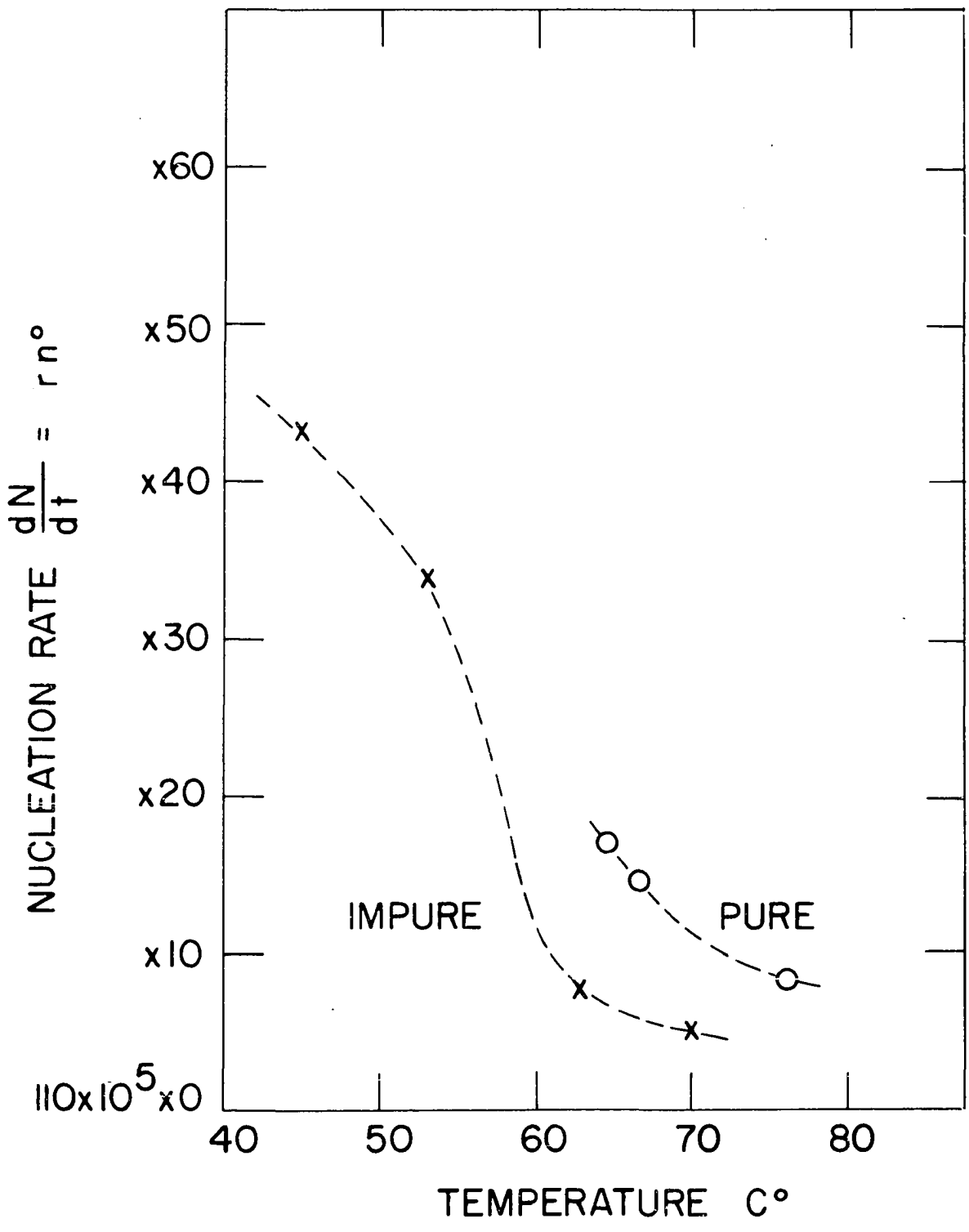
NUCLEATION RATE $\frac{dN}{dt} = rn^{\circ}$
x60
x50
x40
x30
x20
x10
110x10^5x0
IMPURE
PURE
40
50
60
70
80
TEMPERATURE C°

Figure 8. Semi-log plot of population density versus size for crystallization of semihydrate from 49.5% phosphoric acid (35.8% P_2O_5) pure feeds

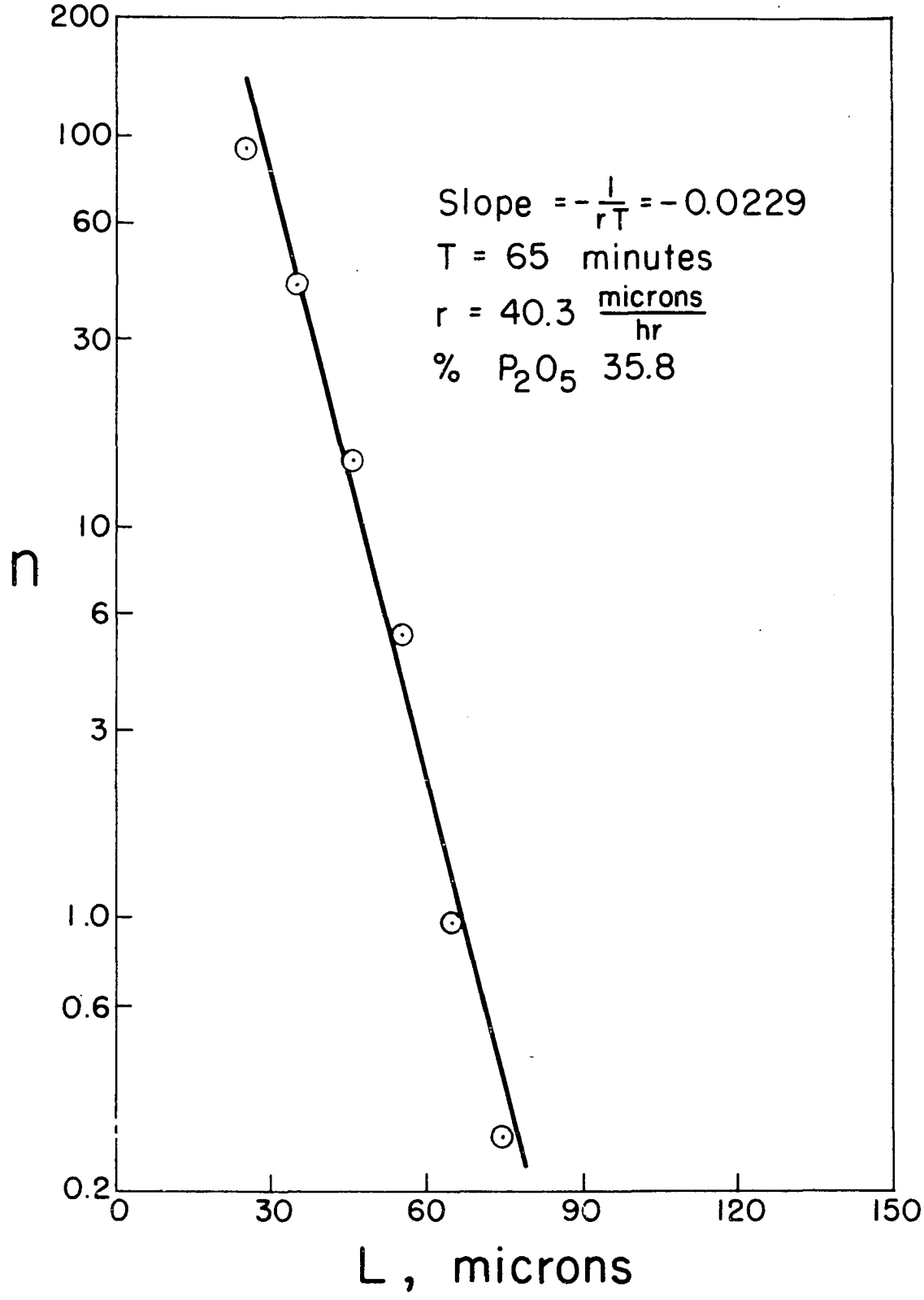
200
100
60
30
10
6
3
1.0
0.6
0.2
n
0
30
60
90
120
150
L, microns
Slope $= -\frac{1}{rT} = -0.0229$
T = 65 minutes
r = 40.3 $\frac{\text{microns}}{\text{hr}}$
% P_2O_5 35.8

Figure 9. Semi-log plot of population density versus size for crystallization of semihydrate from 53.8% phosphoric acid (39% P_2O_5) pure feeds

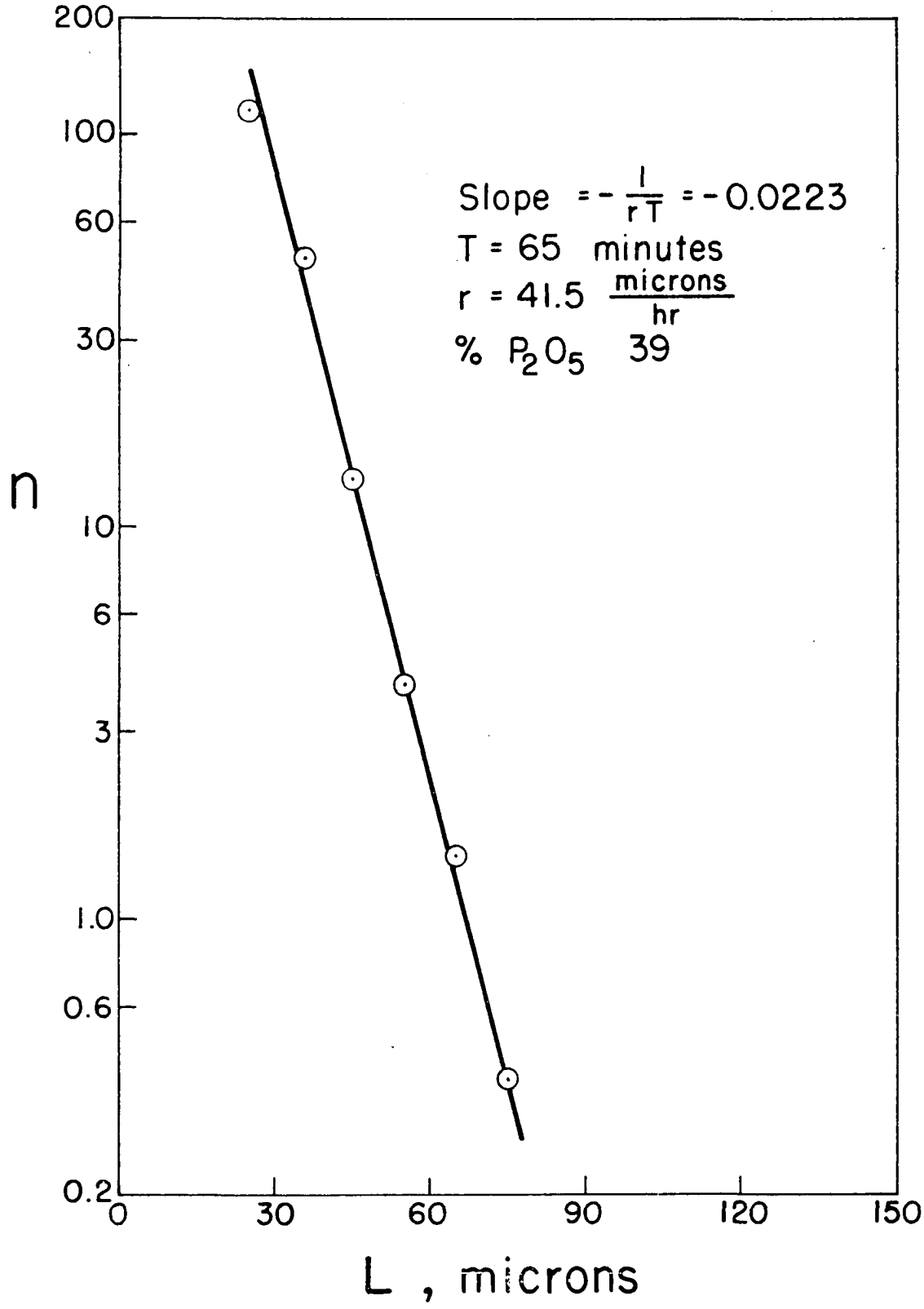
200
100
60
30
10
6
3
1.0
0.6
0.2
n
0
30
60
90
120
150
L , microns
Slope = $-\frac{1}{rT}$ = -0.0223
T = 65 minutes
r = 41.5 $\frac{\text{microns}}{\text{hr}}$
% P_2O_5 39

Figure 10. Semi-log plot of population density versus size for crystallization of semihydrate from 58% phosphoric acid (42% P_2O_5) pure feeds

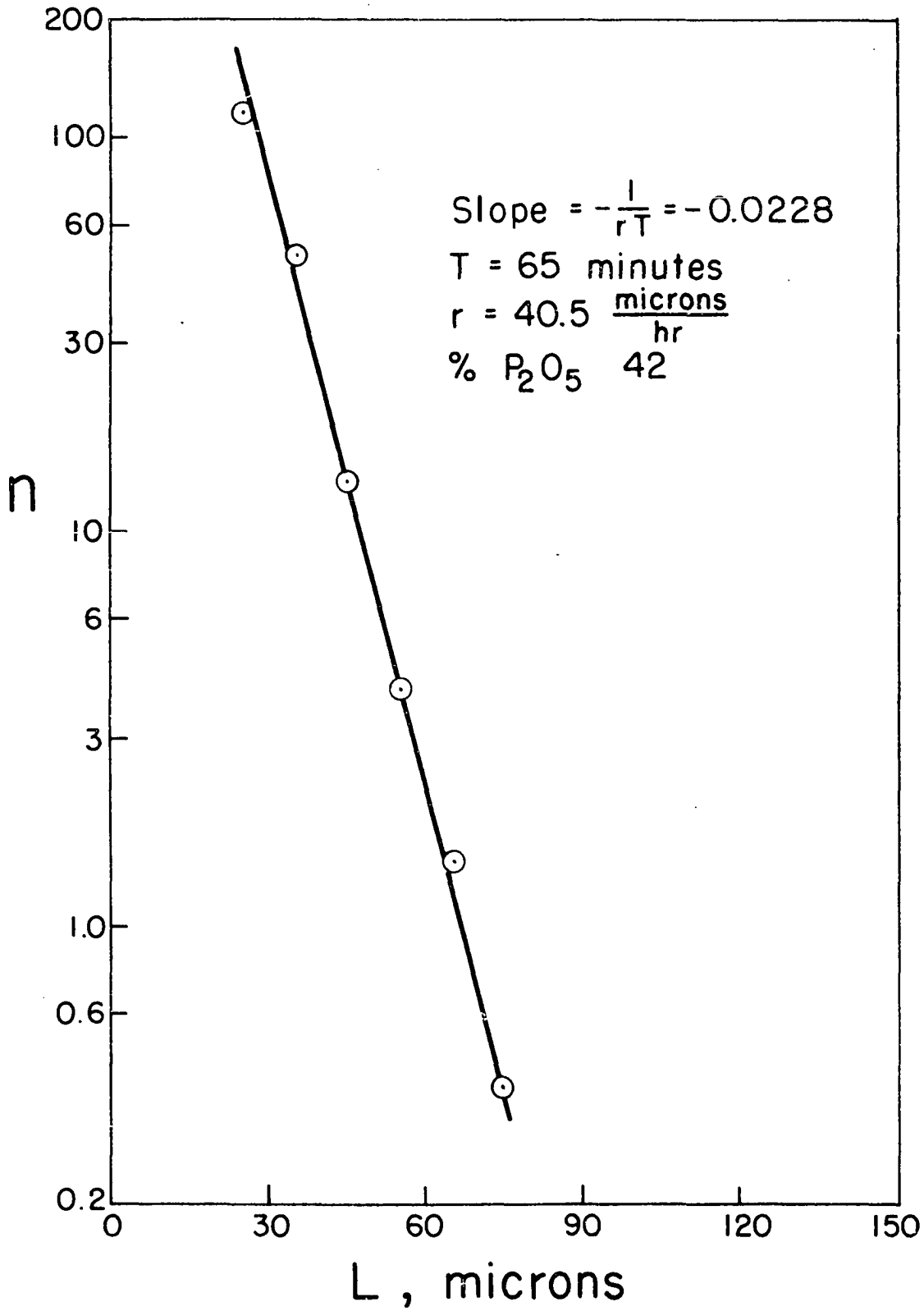
200
100
60
30
10
6
3
1.0
0.6
0.2
n
Slope = $-\frac{1}{rT}$ = -0.0228
T = 65 minutes
r = 40.5 $\frac{\text{microns}}{\text{hr}}$
% P_2O_5 42
0
30
60
90
120
150
L , microns

Extension of this range was not possible because of the possibilities of crystallizing other forms of calcium sulphate.

Growth and Nucleation: Kinetic Orders for Semihydrate

Pure feeds

Three steady state runs were carried out using reagent grade feeds, at constant temperature of 70 C°, and an acid concentration of 42% P_2O_5. From the Coulter Counter analyses of steady state crystal distribution, population densities at corresponding sizes were calculated. Figures 11, 12, and 13 present the plots of the steady state equation, Equation 1. The n° and r data obtained from these plots are summarized in Table 4 along with pertinent operating conditions and were used with Equation 13 to obtain a plot of log n° versus log r as shown in Figure 14. A straight line with a slope of 1.8 was obtained. The general kinetic equation, Equation 13, can now be written as follows for the crystallization of semihydrate from the pure feeds,

$$n^{\circ} = K\, r^{1.8}$$

and Equation 12 becomes

$$\frac{dW}{dt} = K\, r^{2.8}$$

It is of interest to note here that as the residence time increases the intercept on the "y" axis, Figures 11, 12, and 13, decreases. This obviously means that as the residence time is increased, nucleation rate decreases, implying that supersaturation decreases. A decrease in supersaturation causes a decrease in the growth rate also. However, since the crystals remain in the crystallizer for a longer period the size of the

Figure 11. Semi-log plot of population density versus size for residence time T = 12 minutes pure feeds

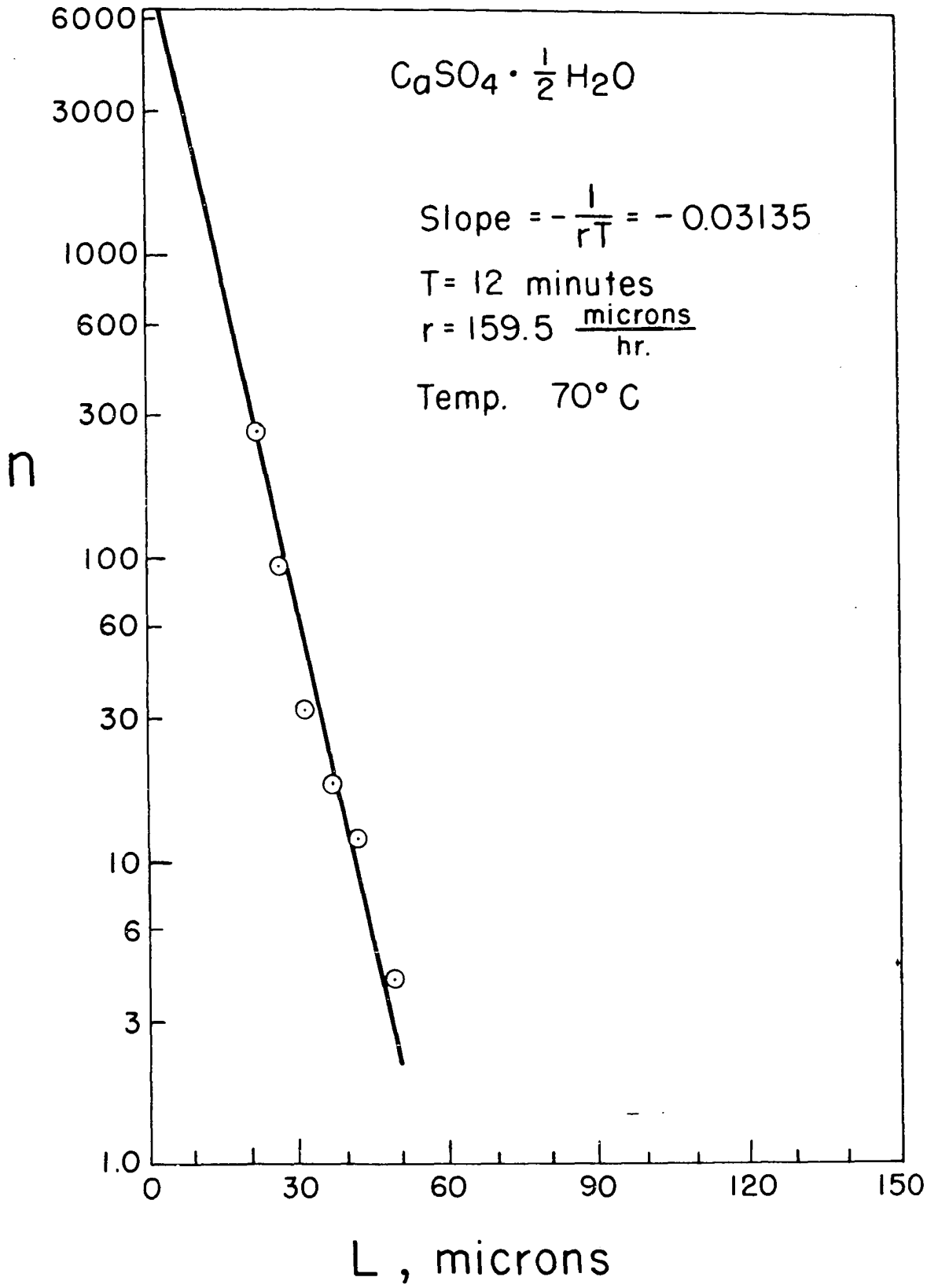
$CaSO_4 \cdot \frac{1}{2} H_2O$
Slope $= -\frac{1}{rT} = -0.03135$
T = 12 minutes
r = 159.5 microns/hr.
Temp. 70° C
n
6000
3000
1000
600
300
100
60
30
10
6
3
1.0
0
30
60
90
120
150
L , microns

Figure 12. Semi-log plot of population density versus size for residence time T = 29.5 minutes pure feeds

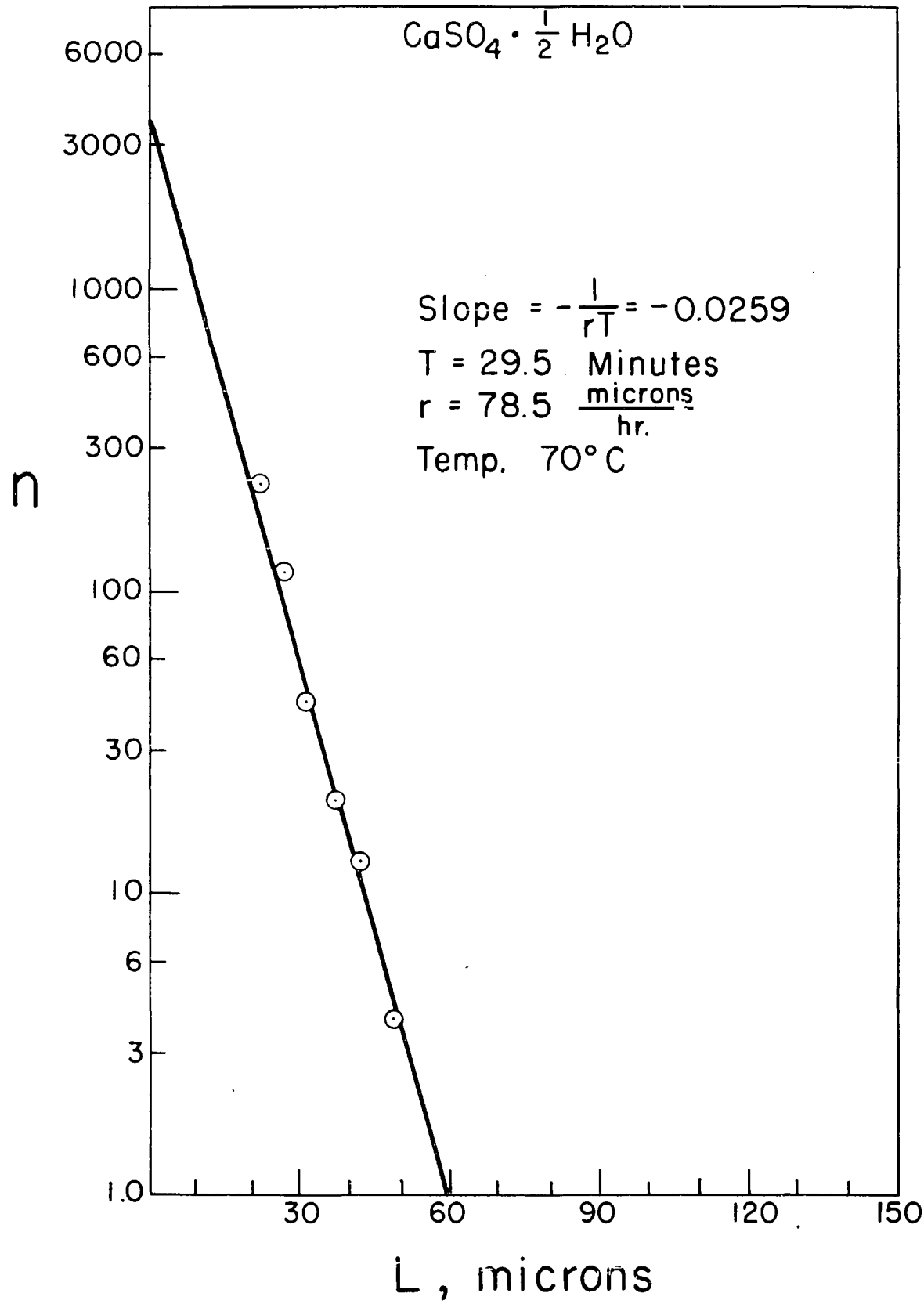
$CaSO_4 \cdot \frac{1}{2} H_2O$
Slope = $-\frac{1}{rT} = -0.0259$
T = 29.5 Minutes
r = 78.5 $\frac{\text{microns}}{\text{hr.}}$
Temp. 70° C
n
6000
3000
1000
600
300
100
60
30
10
6
3
1.0
30
60
90
120
150
L, microns

Figure 13. Semi-log plot of the population density versus size for residence time T = 45 minutes pure feeds

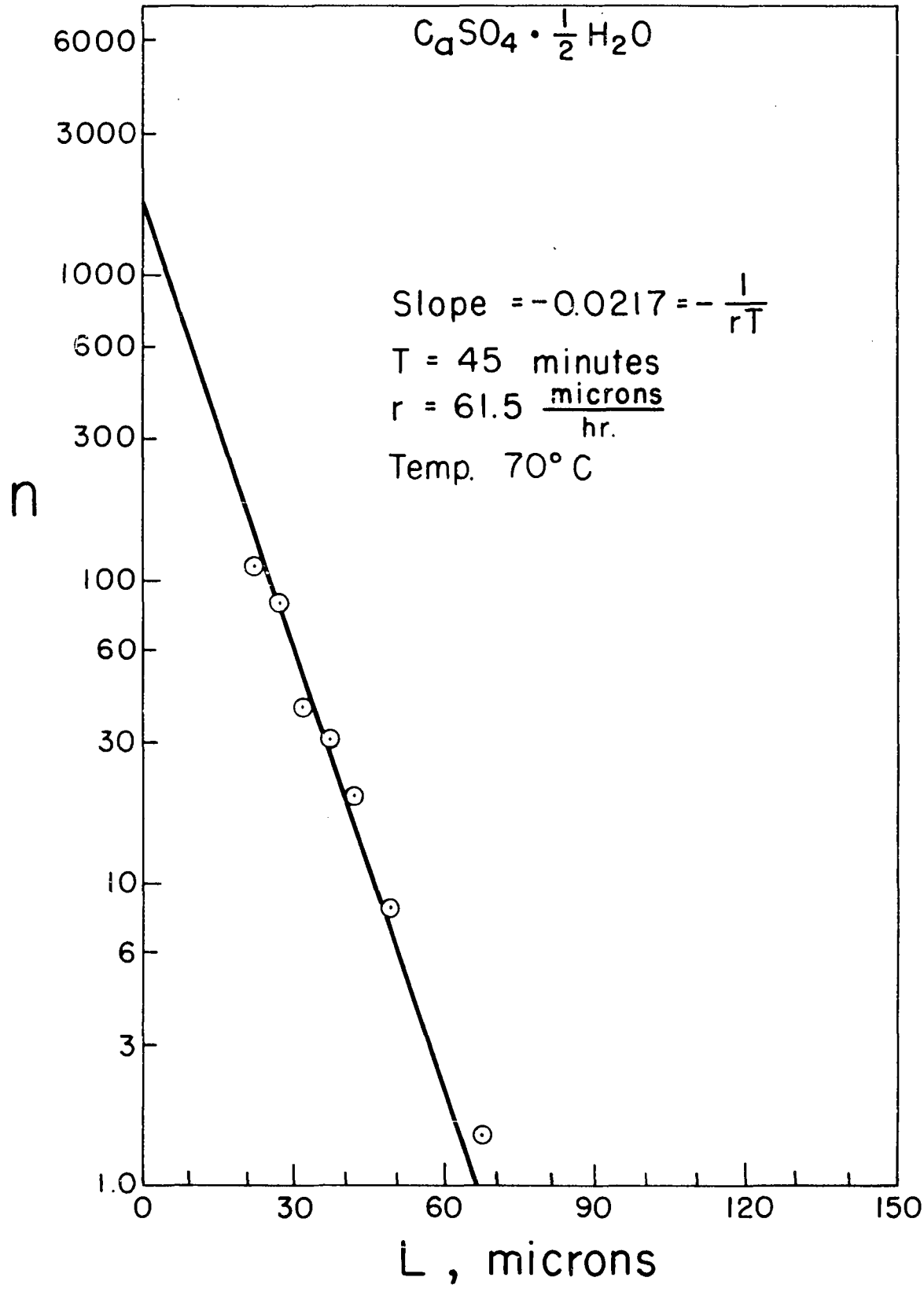
$CaSO_4 \cdot \frac{1}{2} H_2O$
Slope $= -0.0217 = -\frac{1}{rT}$
T = 45 minutes
r = 61.5 $\frac{\text{microns}}{\text{hr.}}$
Temp. 70° C
n
6000
3000
1000
600
300
100
60
30
10
6
3
1.0
0
30
60
90
120
150
L, microns

Figure 14. Log-log plot of nuclei population density versus steady state growth rate of semihydrate from pure phosphoric acid

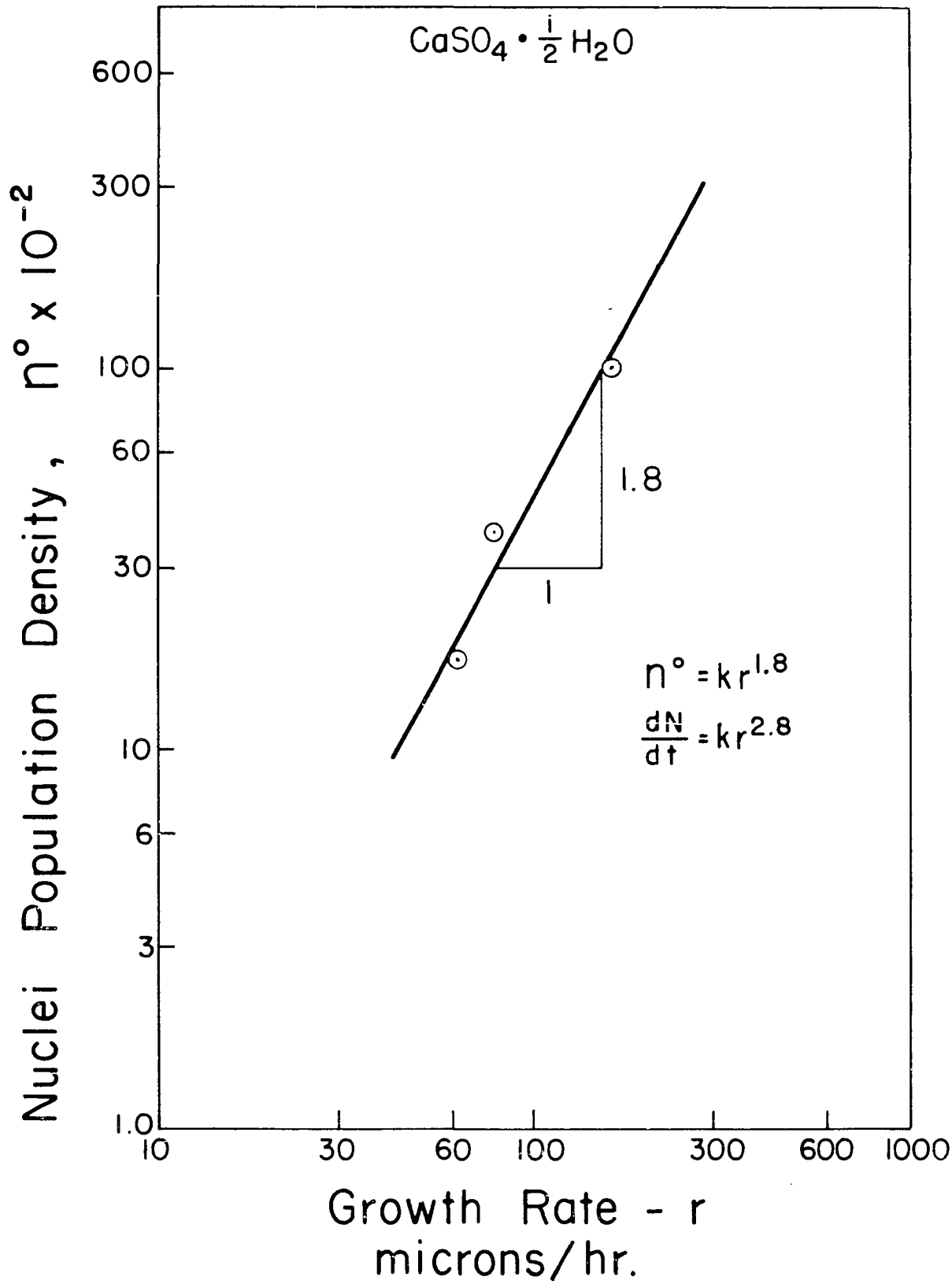
$CaSO_4 \cdot \frac{i}{2} H_2O$
600
300
100
60
30
10
6
3
1.0
Nuclei Population Density, $n^\circ \times 10^{-2}$
1.8
1
$n^\circ = kr^{1.8}$
$\frac{dN}{dt} = kr^{2.8}$
10
30
60
100
300
600
1000
Growth Rate - r
microns/hr.

Table 4. Variation of residence time - pure feeds

Run No.	Temp C°	% suspension density	Residence time T minutes	Growth rate r microns per hour	n^o
21	70	0.442	12	159.5	10000
22	70	0.410	29.5	78.5	3700
23	70	0.462	45	61.5	1700

largest crystal in the crystallizer increases. This results in an improvement in the size distribution because there is a reduction in the number of the smaller size crystals and an increase in the number of larger size crystals. Steady state data of Figures 11 and 13 are combined in Figure 15 to reveal this effect more precisely.

Impure feeds

Five steady state runs, shown in Table 5, were carried out using impure feeds, that is feeds prepared using commercial wet-process acid. Residence time was varied by changing the height of the withdrawal tube. The population density versus size plots are presented in Figures 16, 17, 18, 19, and 20. A plot of log n^o versus log r, Figure 21, was made as before. A straight line having a slope of 1.6 was obtained. The general kinetic equation for crystallization of semihydrate from impure materials can now be written as,

$$n^o = K\, r^{1.6}$$

and nucleation rate equation is

$$\frac{dN}{dt} = K\, r^{2.6}$$

Figure 15. Comparison of the size distributions for residence times T = 12 and T = 45 minutes pure feeds

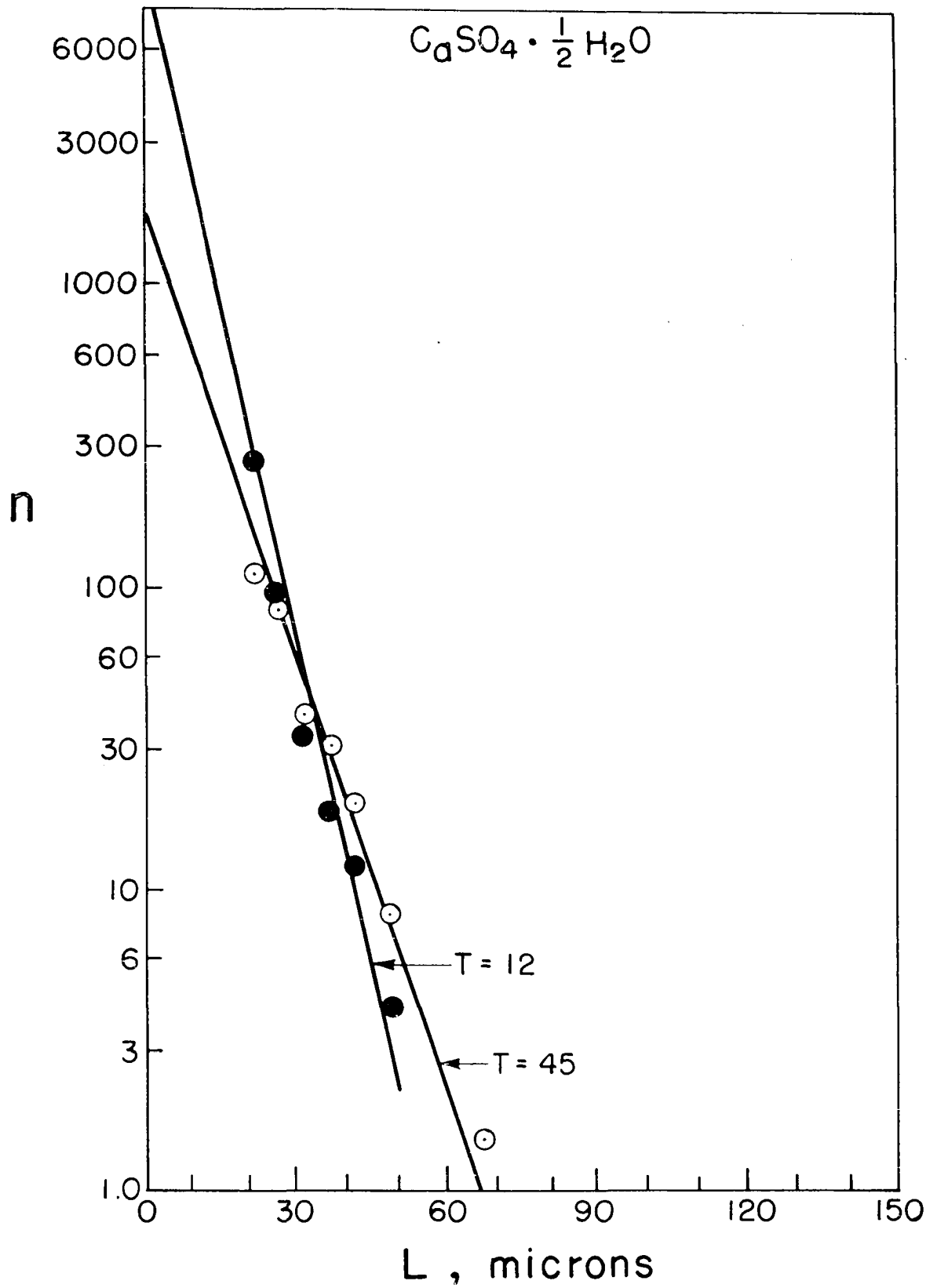
$CaSO_4 \cdot \frac{1}{2} H_2O$
6000
3000
1000
600
300
100
60
30
10
6
3
1.0
n
T = 12
T = 45
0
30
60
90
120
150
L , microns

Figure 16. Semi-log plot of population density versus size for residence time T = 6.88 minutes impure feeds

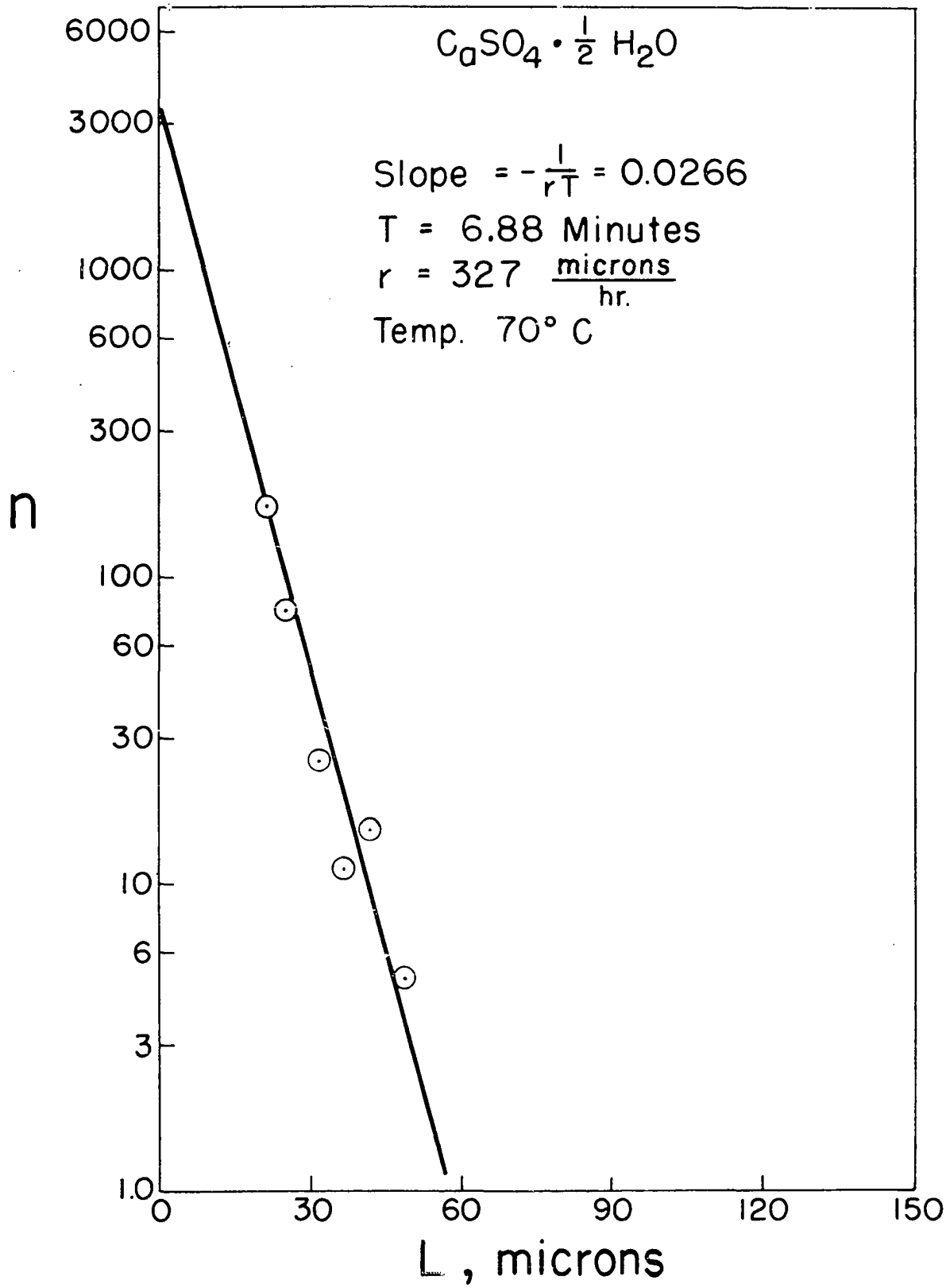
$CaSO_4 \cdot \frac{1}{2} H_2O$
Slope $= -\frac{1}{rT} = 0.0266$
T = 6.88 Minutes
r = 327 microns/hr.
Temp. 70° C
n
6000
3000
1000
600
300
100
60
30
10
6
3
1.0
0
30
60
90
120
150
L, microns

Figure 17. Semi-log plot of population density versus size for residence time T = 11.6 minutes impure feeds

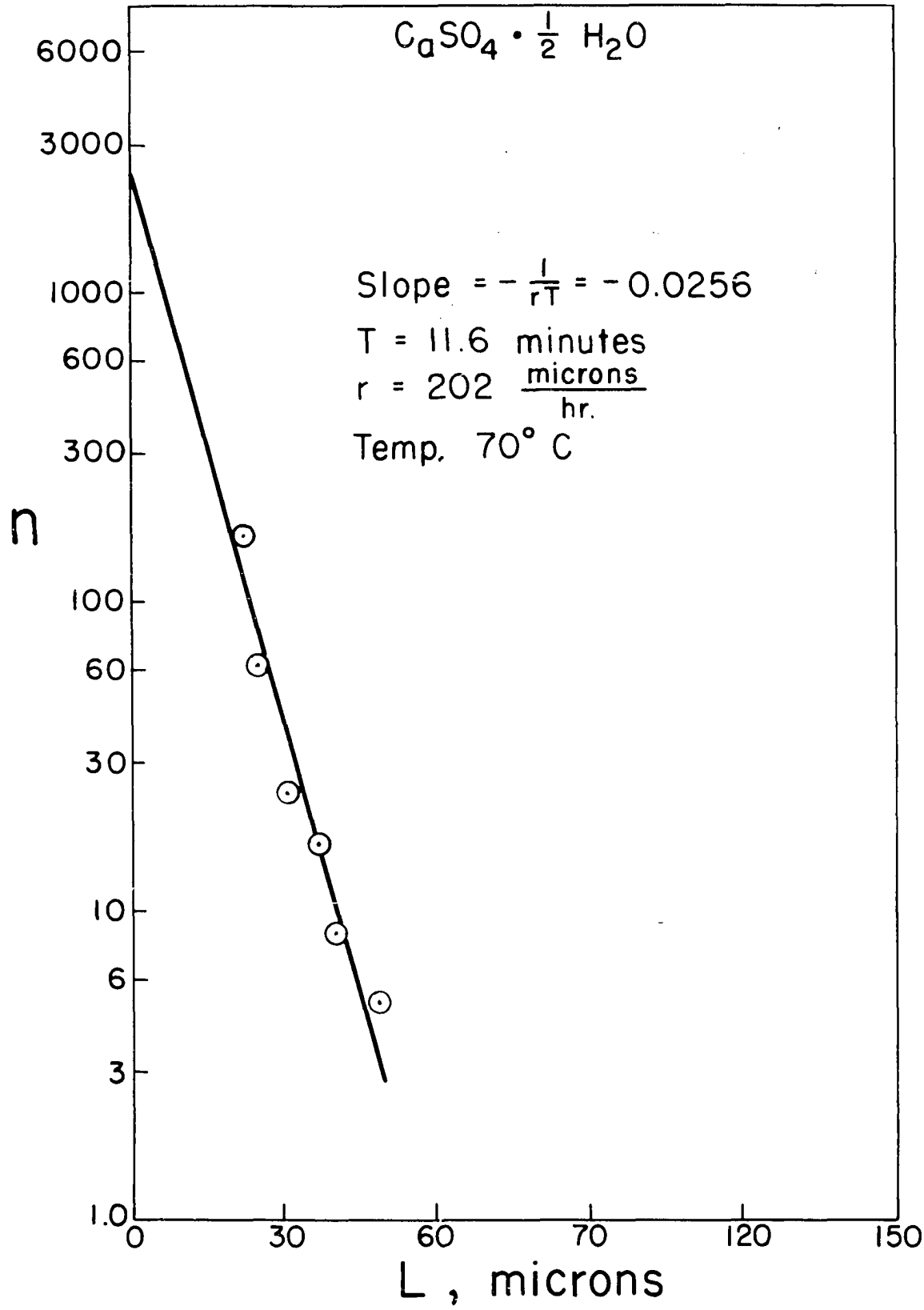
$CaSO_4 \cdot \frac{1}{2} H_2O$
Slope $= -\frac{1}{rT} = -0.0256$
T = 11.6 minutes
r = 202 microns/hr.
Temp. 70° C
n
6000
3000
1000
600
300
100
60
30
10
6
3
1.0
0
30
60
70
120
150
L, microns

Figure 18. Semi-log plot of population density versus size for residence time T = 14.4 minutes impure feeds

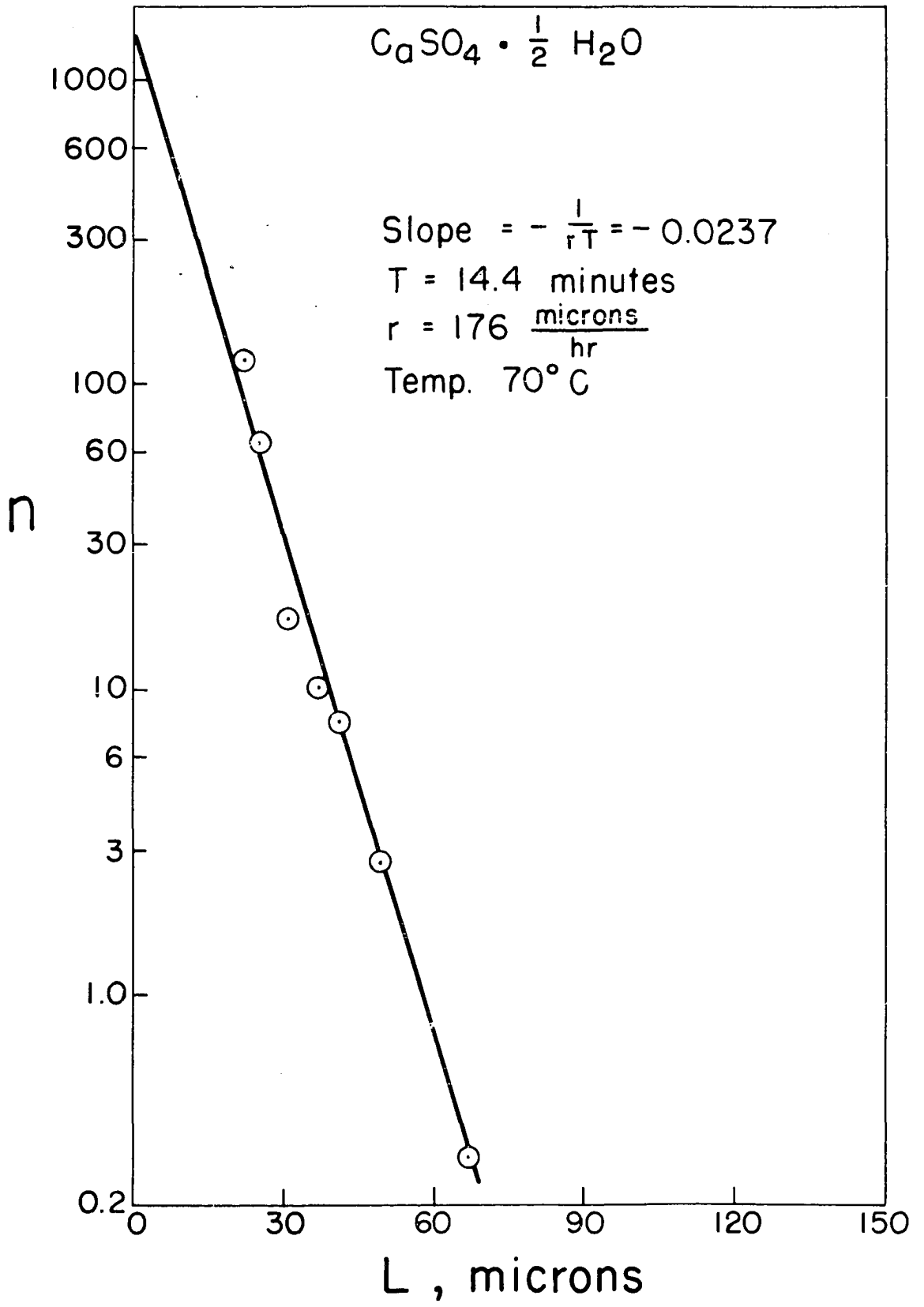
$CaSO_4 \cdot \frac{1}{2} H_2O$
Slope $= -\frac{1}{rT} = -0.0237$
T = 14.4 minutes
r = 176 $\frac{\text{microns}}{\text{hr}}$
Temp. 70° C
n
1000
600
300
100
60
30
10
6
3
1.0
0.2
0
30
60
90
120
150
L , microns

Figure 19. Semi-log plot of population density versus size for residence time T = 14.1 minutes impure feeds

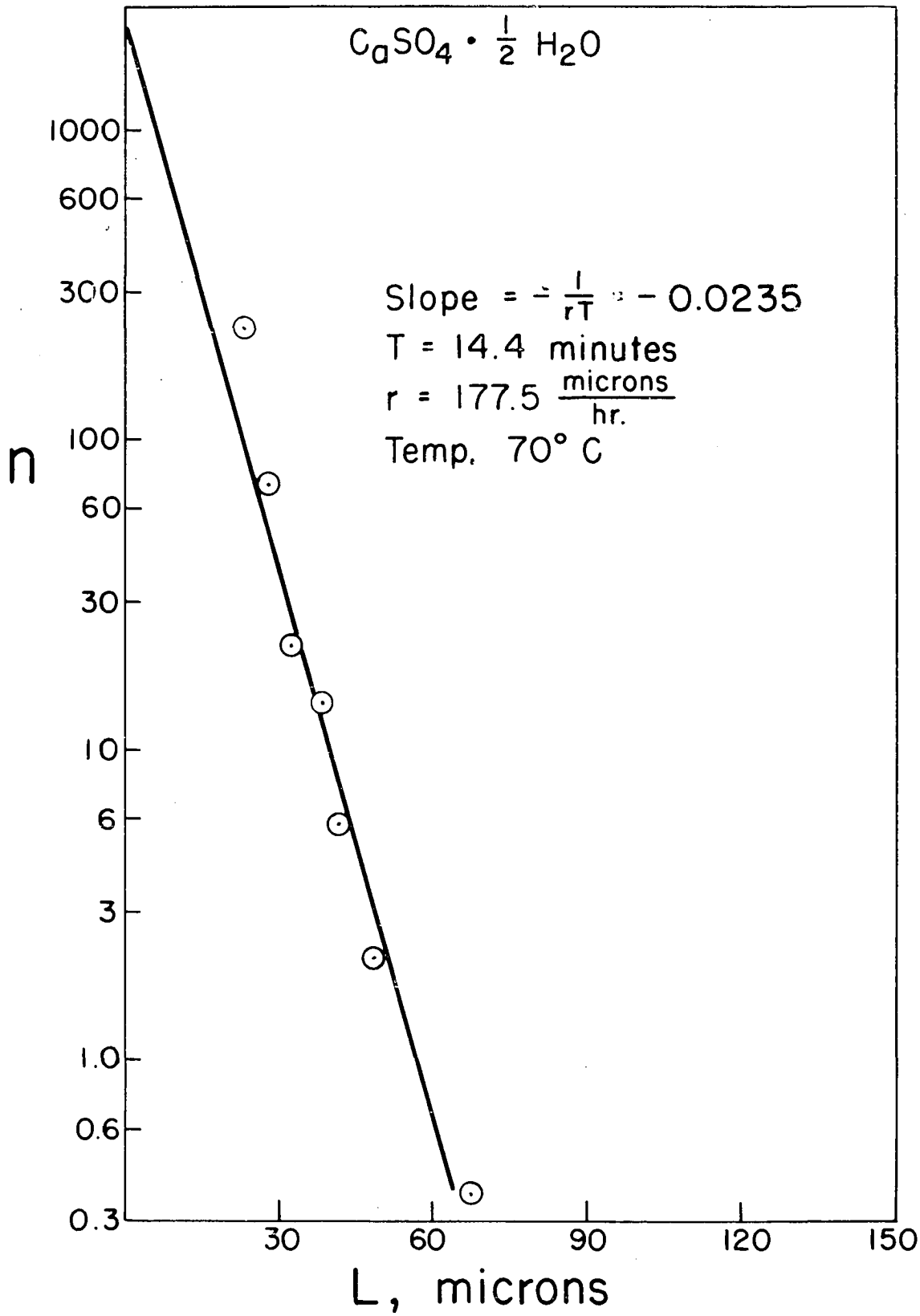
$CaSO_4 \cdot \frac{1}{2} H_2O$
Slope = $-\frac{1}{rT}$ = - 0.0235
T = 14.4 minutes
r = 177.5 microns/hr.
Temp. 70° C
n
1000
600
300
100
60
30
10
6
3
1.0
0.6
0.3
30
60
90
120
150
L, microns

Figure 20. Semi-log plot of population density versus size for residence time T = 37.5 minutes impure feeds

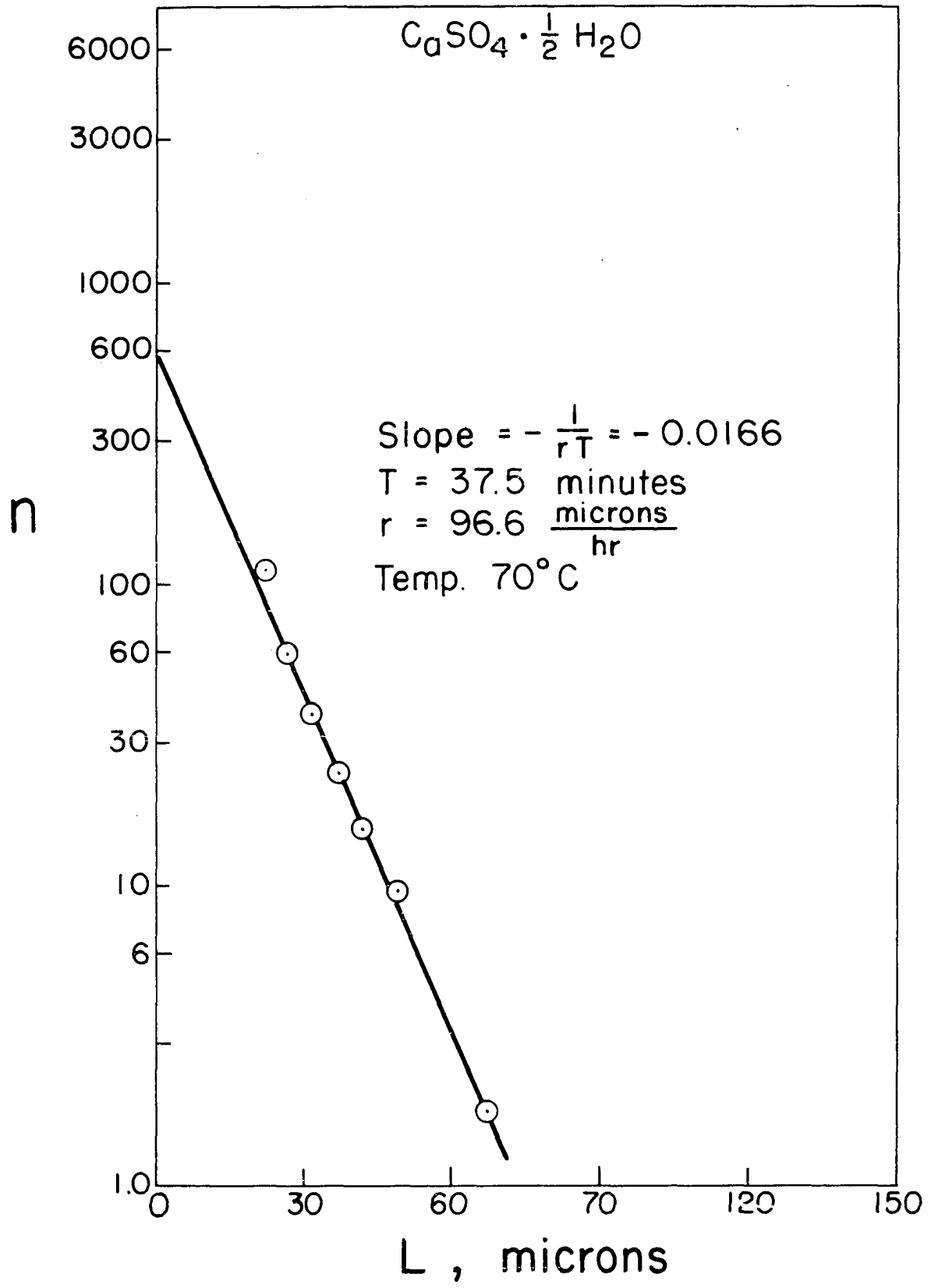
$CaSO_4 \cdot \frac{1}{2} H_2O$
Slope $= -\frac{1}{rT} = -0.0166$
T = 37.5 minutes
r = 96.6 microns/hr
Temp. 70° C
n
6000
3000
1000
600
300
100
60
30
10
6
1.0
0
30
60
70
120
150
L , microns

Figure 21. Log-log plot of nuclei population density versus steady state growth rate for semihydrate in impure phosphoric acid

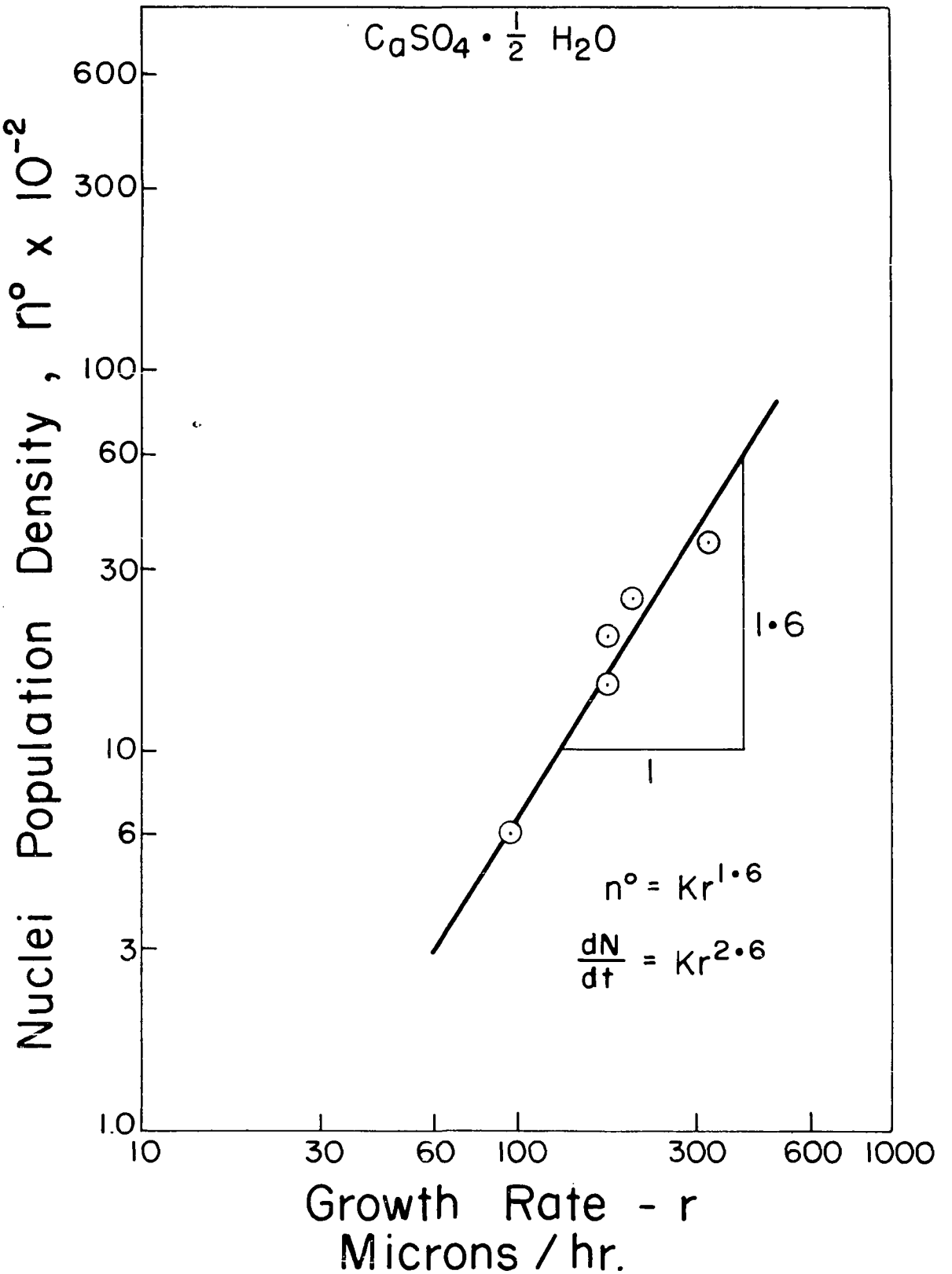
$CaSO_4 \cdot \frac{1}{2} H_2O$
Nuclei Population Density , $n^o \times 10^{-2}$
600
300
100
60
30
10
6
3
1.0
10
30
60
100
300
600
1000
1·6
1
$n^o = Kr^{1·6}$
$\frac{dN}{dt} = Kr^{2·6}$
Growth Rate - r
Microns / hr.

Table 5. Variation of residence time - impure feeds

Run No.	% suspension density	Temperature = 70 C° Residence time T minutes	Growth rate r microns per hour	% P_2O_5 in crystals	n^o
25	0.682	6.88	327.0	0.04	3500
26	0.647	11.60	202.0	0.04	2600
28	0.568	14.40	184.0	0.05	1500
30	0.562	14.40	177.5	0.05	2000
27	0.653	37.50	99.5	0.04	600

A comparison of these equations with the kinetic equations obtained earlier for pure feeds shows that wet-process impurities in the feeds do not have a significant effect on the kinetic order. Figure 22 summarizes the effect of draw down time on growth rate for pure and impure feeds. It is of interest to note the explosive nature of the increase in the growth rate as draw down time is decreased. It can also be observed that the impure acid increases the growth rate, but decreases the population density of nuclei, as may be observed in Table 5 and thus the impure acid crystals have an enhanced size distribution, even though the kinetic order is not appreciably different.

Suspension Density

Equation 32 presents a method for determining the fundamental mechanism for nucleation. That is, is the nucleation mechanism homogeneous or heterogeneous? By holding all other operating conditions constant and

Figure 22. Plot of growth rate versus draw down time (residence time) T for pure and impure feeds

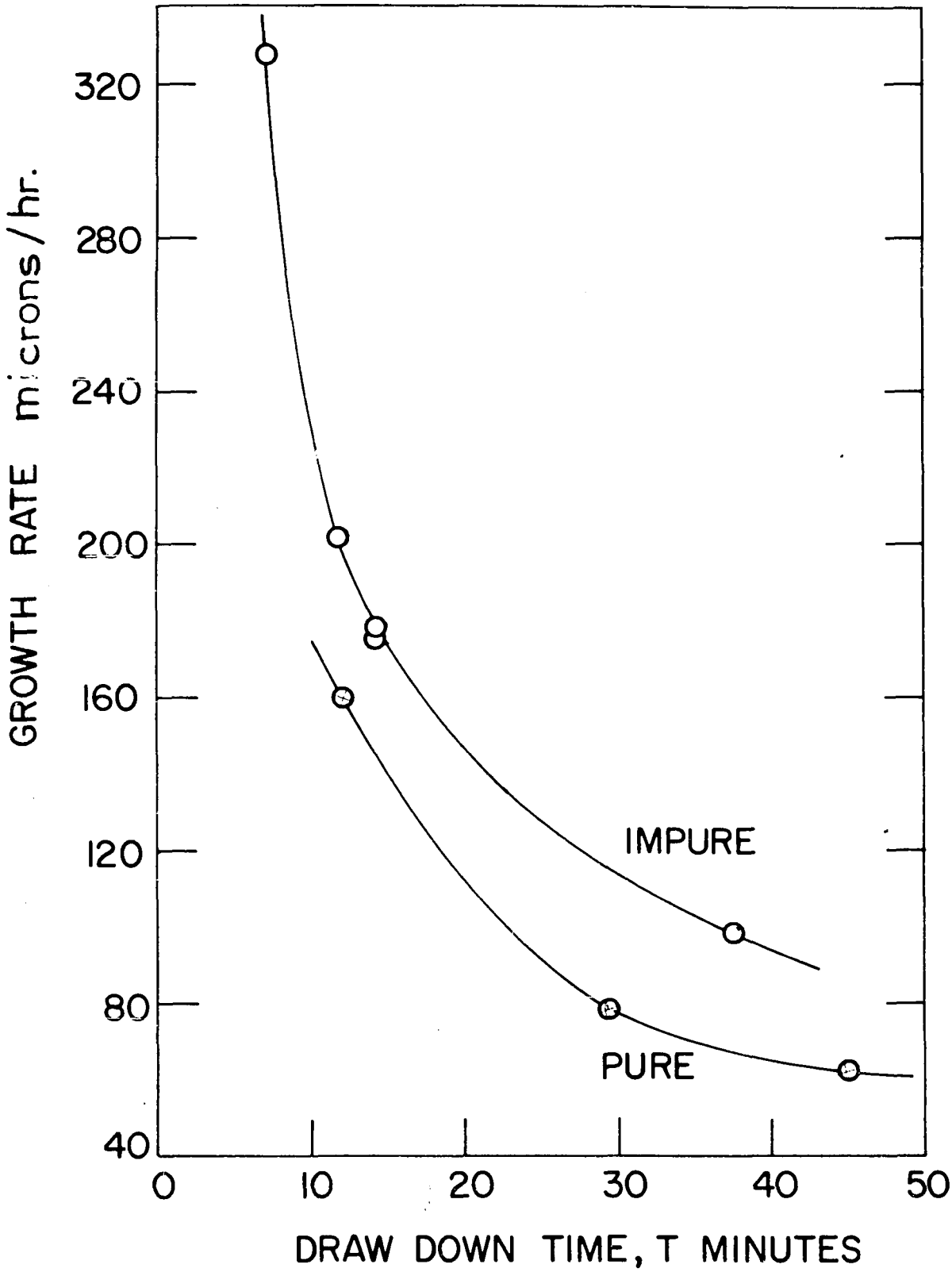
GROWTH RATE microns/hr.
320
280
240
200
160
120
80
40
0
10
20
30
40
50
DRAW DOWN TIME, T MINUTES
IMPURE
PURE

by varying suspension density in a known fashion, the kinetic order of the suspension density parameter may be determined. If "d" is zero, the mechanism is homogeneous, if "d" is not zero, the mechanism is heterogeneous.

Two steady state runs, shown in Table 6, were carried out with different constant suspension densities. Growth rate and nuclei population density data were obtained from Figures 23 and 24. The nuclei population densities were arbitrarily based on 9.1×10^{-4} grams of crystals. Their numerical values were corrected to the actual value of the suspension density, based on a unit suspension volume.

Table 6. Variation of suspension density

Run No.	Temp C°	% suspension density	Residence time T minutes	Growth rate r microns per hour
47	70	1.525	40.8	78.3
48	70	3.760	42.1	91.0

Equation 34 presents a method for determining the effect of suspension density from these experimental data. Since "a/b -1" (= 1.8) has been previously determined from residence time experiments, one may evaluate directly the constant "d". Such a calculation, shown in Table 7, indicates that the value of "d" is zero. Thus the mechanism is homogeneous. An additional calculation by Equation 30 substantiates this conclusion.

The data of Figures 23 and 24 also present a visual means of emphasizing the effect of suspension density for a homogeneous nucleation

Figure 23. Semi-log plot of population density versus size for suspension density ϕ = 1.525% pure feeds

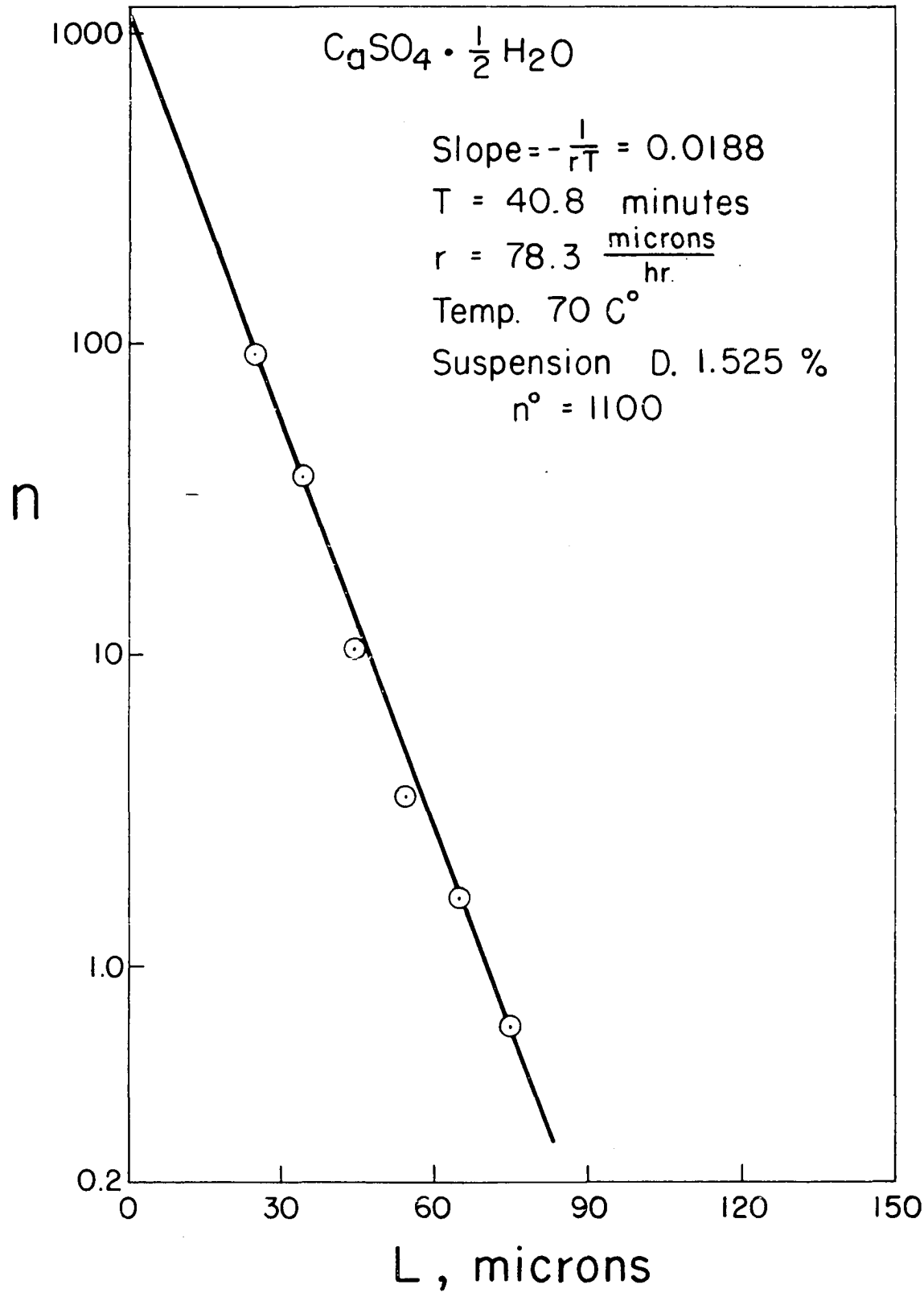
$CaSO_4 \cdot \frac{1}{2} H_2O$
Slope = $-\frac{1}{rT}$ = 0.0188
T = 40.8 minutes
r = 78.3 microns/hr.
Temp. 70 C°
Suspension D. 1.525 %
n° = 1100
n
1000
100
10
1.0
0.2
0
30
60
90
120
150
L, microns

Figure 24. Semi-log plot of population density versus size for suspension density ϕ = 3.76% pure feeds

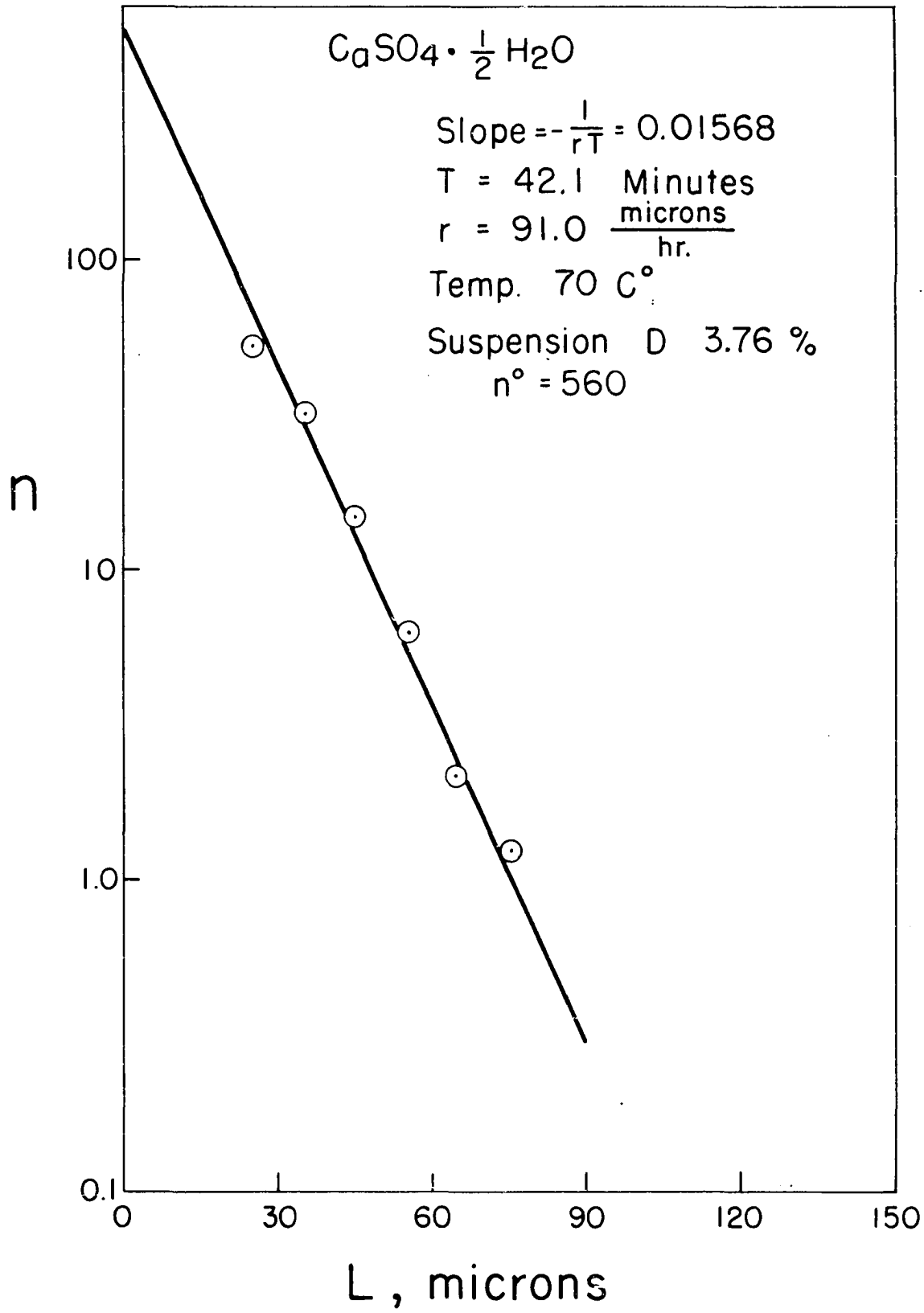
$CaSO_4 \cdot \frac{1}{2} H_2O$
Slope $= -\frac{1}{rT} = 0.01568$
T = 42.1 Minutes
r = 91.0 microns/hr.
Temp. 70 C°
Suspension D 3.76 %
n° = 560
n
100
10
1.0
0.1
0
30
60
90
120
150
L , microns

Table 7. Determination of nucleation mechanism by variation of suspension density calculations

No.	% suspension density	Growth rate r microns per hour	Actual nuclei population density n^o	$\frac{n_1^o}{n_2^o}=\left(\frac{\phi_1}{\phi_2}\right)^{d=0}\left(\frac{r_1}{r_2}\right)^{1.8}$		$\frac{r_1}{r_2}=\left(\frac{\phi_1}{\phi_2}\right)^{1/1.58}$	
1[a]	3.760	91.0	2.315×10^5				
				1.2550	1x1.308	1.1610	1.1685
2	1.525	78.3	1.845×10^5				

[a] 1 and 2 correspond to run Nos. 47 and 48 respectively

process on the crystal size distribution. These data are redrawn on a combined graph, Figure 25. For the same weight of crystal, the distribution resulting from a higher suspension density has been enhanced, resulting in fewer nuclei, as observed by a comparison of the two straight lines. Moreover the growth rate for the higher suspension is numerically larger than that for the smaller suspension. Thus the crystallization of calcium sulfate as semihydrate should be carried out at as high a suspension density as possible.

This observation assumes that the crystallizer would be mixed suspension, mixed product removal type. In practice, however, there are limitations which do not permit MSMPR conditions. The factors that are prohibitive to higher suspension density are 1) sparing solubility of calcium sulphate in the mother liquor, 2) inability of the present day equipment to achieve perfect mixing economically in large size crystallizers, 3) high concentrations of feed creating localized zones of

Figure 25. Comparison of size distributions obtained for suspension densities of ϕ = 1.525% and ϕ = 3.760% pure feeds

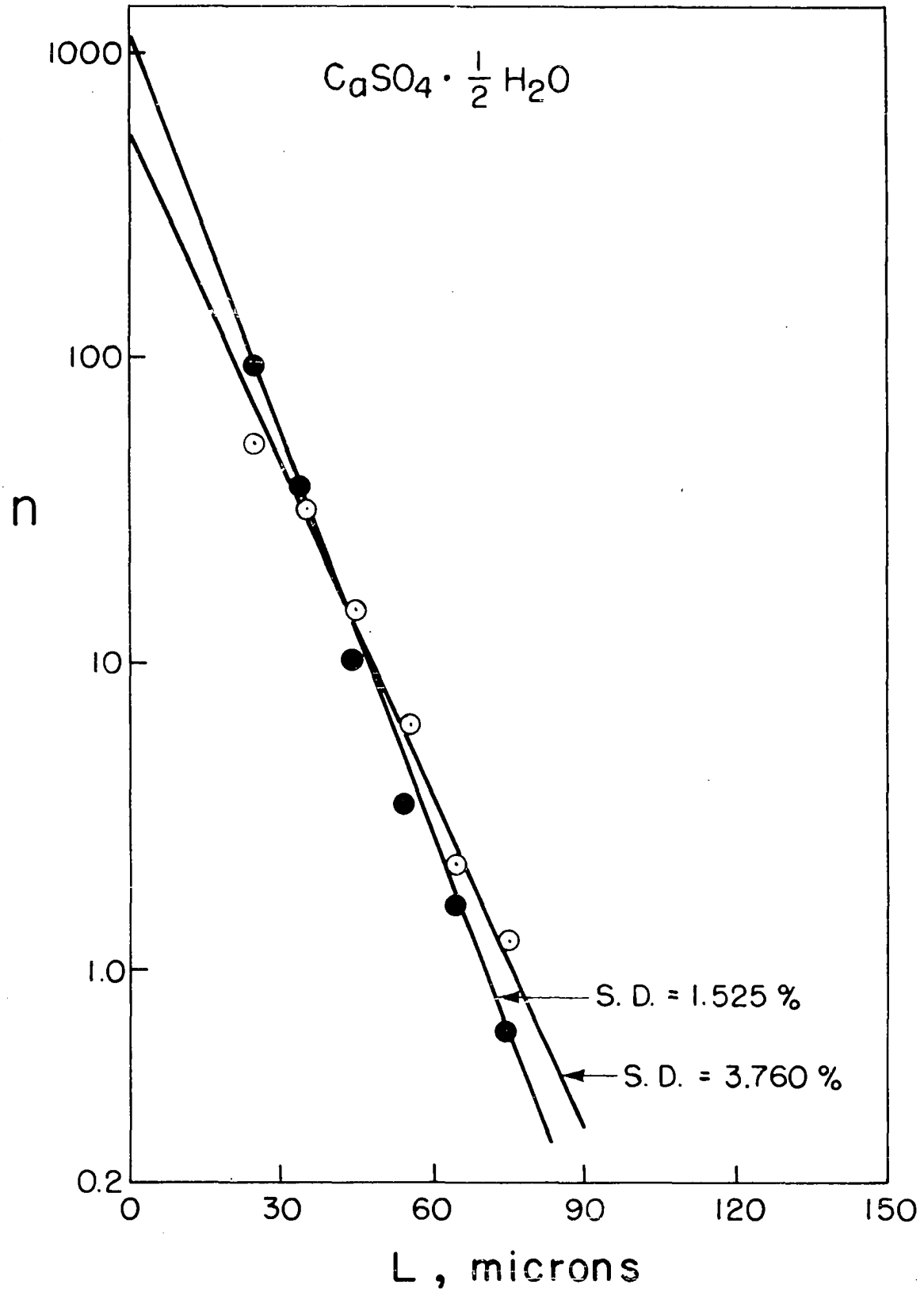
$CaSO_4 \cdot \frac{1}{2} H_2O$
1000
100
10
1.0
0.2
n
0
30
60
90
120
150
L , microns
S. D. = 1.525 %
S. D. = 3.760 %

extremely high supersaturation, 4) common ion effect causing drastic reductions in the solubility of calcium sulphate, 5) high density and viscosity of the mother liquor, 6) increased sluggishness of the suspension, brought out by higher suspension density, and 7) difficulties in pumping and problems associated with settling of solids in the equipment and piping, etc. Under these conditions advantages of higher suspension density would be lost, and on the contrary, there would be heavy nucleation and control difficulties. This effect was also observed by Randolph (27). Consequently a practical limit to the suspension density exists beyond which the advantages of higher suspension density are lost. Commercial processes in use today employ recirculation of the slurry and mother liquor in the order of 20 times the feed rate to achieve proper mixing and crystallization (37).

Habit of Semihydrate Crystals and P_2O_5 Loss

It was predicted in the theoretical considerations that increase in Ca^{++} ion concentration (i.e. monocalcium phosphate concentration) in the crystallizer would decrease the length of the crystals. Three steady state runs, Table 8, using impure feeds were carried out with different Ca^{++} ion concentration, varied by decreasing sulfuric acid feed rate. This affected the residence time slightly; however, it was not significant. Figures 26, 27, and 28 show the photomicrographs of the steady state crystals from these runs. A marked decrease in the lengths of these crystals can be noticed as the calcium ion concentration is increased. Thus experimental results substantiate the conclusion of the theoretical discussion on the crystal habit.

Figure 26. Microscopic photograph (X160) of semihydrate crystals of Run No. 15

Figure 27. Microscopic photograph (X160) of semihydrate crystals of Run No. 16

Figure 28. Microscopic photograph (X160) of semihydrate crystals of Run No. 17

Figure 29. Photograph of an individual crystal of Figure 28 showing the end-view (X1000)

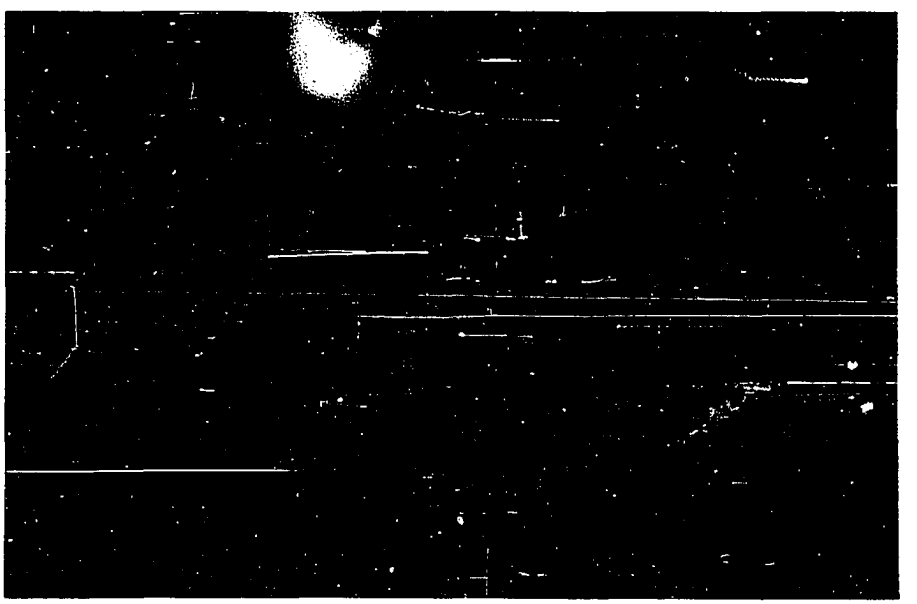

Table 8. Variation of Ca^{++} concentration

Run No.	Temp C°	Calculated % suspension density	Residence time T minutes	Growth rate r microns per hour	% excess[a] Ca^{++}	% P_2O_5 in crystals
15	70	5.81	84.6	63.7	-4.4	0.02
16	70	5.16	89.8	75.7	+22.6	0.02
17	70	3.77	102.8	83.0	+86.7	0.02

[a]Percent excess calcium in the crystallizer over stoichiometric requirement

One effect that was not predicted in the theoretical discussion was the increase in spherulite formation which resulted from increased concentrations of the Ca^{++}. The observed concentrations of calcium ion concentration started at a level in which the SO_4^{--} was in excess of the stoichiometric requirements to one in which the Ca^{++} was in excess. The -4.47% Ca^{++} indicates that SO_4^{--} was in excess whereas the positive number indicates that the amount of Ca^{++} is in excess.

As the excess calcium ion concentration increased from -4.4% to 22.6% the long single crystals turned into spherulites of shorter needles. Further increase in the excess calcium ion concentration from 22.6% to 86.7% increased the number of individual needles attached to the spherulite. However, these needles were so short that it would be inappropriate to refer to them as needles. As the spherulite formation increased, the growth rate was partially reduced because of some unavoidable experimental problem which required an increase in the residence time and a decrease in the suspension density. These operational problems were caused by the

changes made in the sulfuric acid feed rates.

Figure 29 shows the end view of a single needle of the spherulite type crystals of Figure 28. Hexagonal cross sections of semihydrate crystals make them very resistant to breaking during agitation and pumping. During filtration and washing this shape increases the efficiency because of the smaller surface area of contact among the crystals, as compared to the gypsum crystals, which are flat needles with very thin rectangular cross section. Higher specific gravity of semihydrate crystals, compared to specific gravity of gypsum, is also of advantage.

All the experimental runs reported in this dissertation were in a Ca^{++} concentration range of +25% to +50%.

Chemical analysis of crystals was made to determine the total P_2O_5 content. As can be seen from Table 8, an increase in Ca^{++} concentration (i.e. monocalcium phosphate) has no effect on incorporation of the $P\bar{O}_4^{--}$ group in to the crystal structure. Loss of 0.02 percent P_2O_5 in the crystals is negligible. In comparison, P_2O_5 loss due to incorporation in the gypsum crystals has been found (13) up to a maximum of 5.60 percent P_2O_5.

Novel Semihydrate - Phosphoric Acid Process

Discussion

In previous chapters various problems of present day commercial wet-phosphoric acid processes have been discussed. A two stage process, based on fundamental principles of design and crystallization was visualized. Further development of these ideas resulted in a novel semihydrate-phosphoric acid process which possesses many potential economic advantages.

The process is based on the fundamental idea of first reacting rock phosphate with phosphoric acid and then reacting the resultant monocalcium-phosphate with sulfuric acid under conditions which will crystallize calcium sulfate in the form of stable semihydrate. These crystals are easier to filter and wash than the gypsum crystals found in the wet-phosphoric acid process.

Referring to Figure 30, crushed rock phosphate is first reacted with phosphoric acid in a rod mill (3). The major reaction is that of Equation 2. This process continuously reacts the rock and phosphoric acid, resulting in the formation of triple-super-phosphate. Intense mixing, heating and drying inside the mill completes the conversion within a few hours. The mill operates at temperatures higher than 300 °F and requires a residence time of less than two hours (3).

The solid triple-super-phosphate from the rod mill is fed to an extractor in which the monocalcium phosphate is dissolved in phosphoric acid. Recycled phosphoric acid is used in this leaching operation. Sludge, containing silica and various other undissolved impurities, is removed by filtration.

The filtered liquor is fed to the crystallizer. Sulfuric acid is added to react with the dissolved monocalcium phosphate, resulting in the formation of semihydrate crystals. A large amount of the crystallizer's effluent, after being cooled in a flash chamber, is recirculated to dilute the sulfuric acid feed before the acid is introduced to the crystallizer. This dilution will reduce the sulfuric acid concentration, thus reducing the nucleation rate at the feed points.

Figure 30. Material balance and the flow diagram of the proposed process

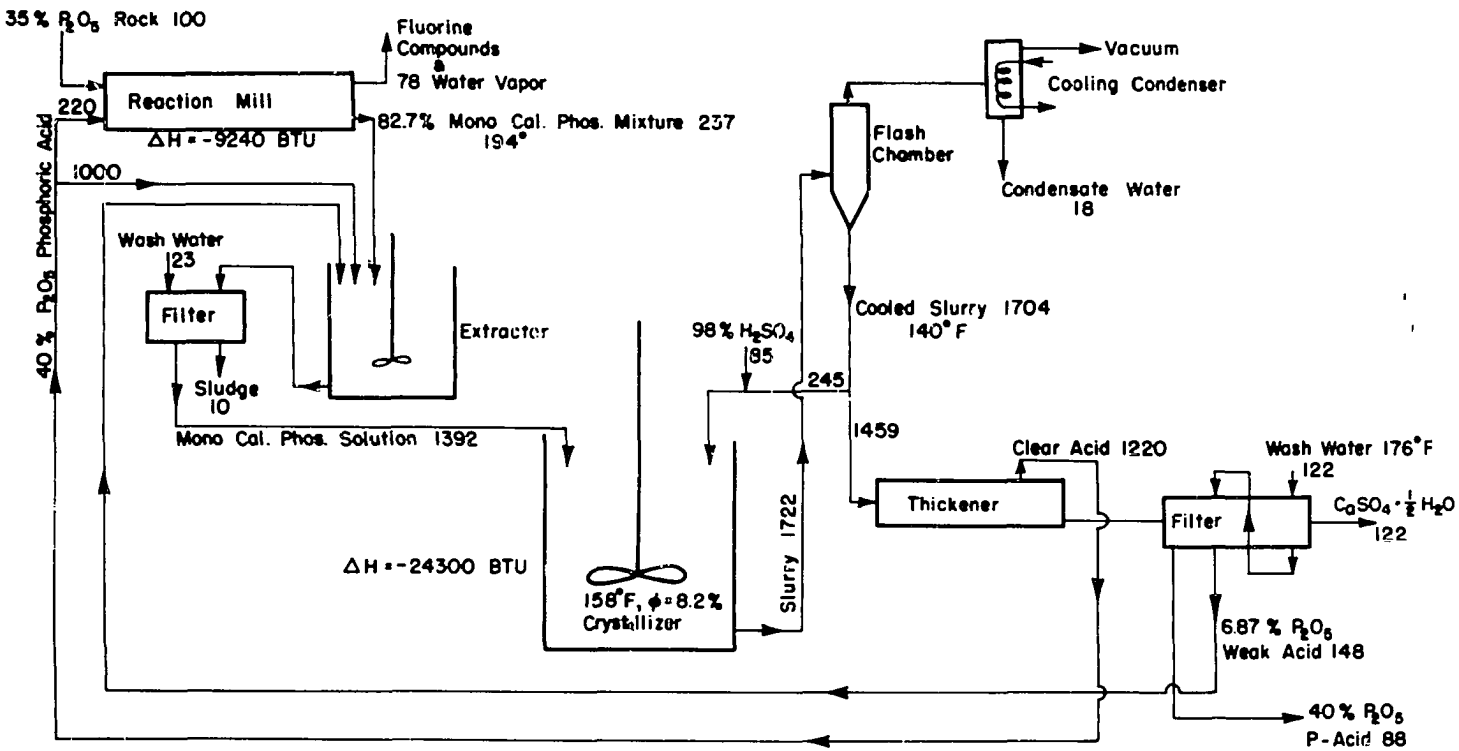
35 % P_2O_5 Rock 100
Fluorine Compounds
78 Water Vapor
Reaction Mill
220
ΔH = -9240 BTU
82.7% Mono Cal. Phos. Mixture 237
194°
1000
40 % P_2O_5 Phosphoric Acid
Wash Water
123
Filter
Sludge
10
Extractor
Mono Cal. Phos. Solution 1392
ΔH = -24300 BTU
158°F, ϕ = 8.2 %
Crystallizer
Slurry 1722
98 % H_2SO_4
185
245
1459
Flash Chamber
Vacuum
Cooling Condenser
Condensate Water
18
Cooled Slurry 1704
140° F
Clear Acid 1220
Thickener
Wash Water 176°F
122
Filter
$CaSO_4 \cdot \frac{1}{2} H_2O$
122
6.87 % P_2O_5
Weak Acid 148
40 % P_2O_5
P-Acid 88

The cooled, concentrated acid from the flash evaporator is fed to a thickener, from which clear phosphoric acid is recycled to the extractor and to the rod mill. The concentrated solids-acid mixture from the thickner is next filtered to remove the semihydrate crystals, resulting in a product acid containing 40% P_2O_5. The crystals are washed, then removed from the system. The wash liquid contains 6.87% P_2O_5 and is recycled to the extractor.

Material balance

Figure 30 also shows an overall material balance for the semihydrate-phosphoric acid process, based on 100 lbs. of phosphate rock feed. A total of 88 lbs. of 40% P_2O_5 product acid and 122 lbs. of semihydrate crystals are produced. In addition to the phosphate rock feed, 85 lbs. of 98% sulfuric acid is required for crystallization plus water requirements for washing solids after filtering.

Fluorine removal

Samples of triple-super-phosphate produced by Boylan and Amin (3) were obtained and analyzed for fluorine content. These data were then plotted as fluorine content versus acidulation ratio, Figure 31. Several conclusions can be drawn from this plot; 1) increase in acidulation ratio increases fluorine removal from triple superphosphate, 2) more fluorine is removed at higher temperatures, 3) increase in residence time increases removal of fluorine.

In the proposed process operating conditions can be selected to optimize the fluorine removal. Higher acidulation ratios can be employed without any disadvantage because the additional acid returns to the

Figure 31. Plot of percent flourine versus acidulation ratio for triple-super-phosphate samples of Boylan and Amin - numbers in rectangles represent the product temperatures in degrees F°

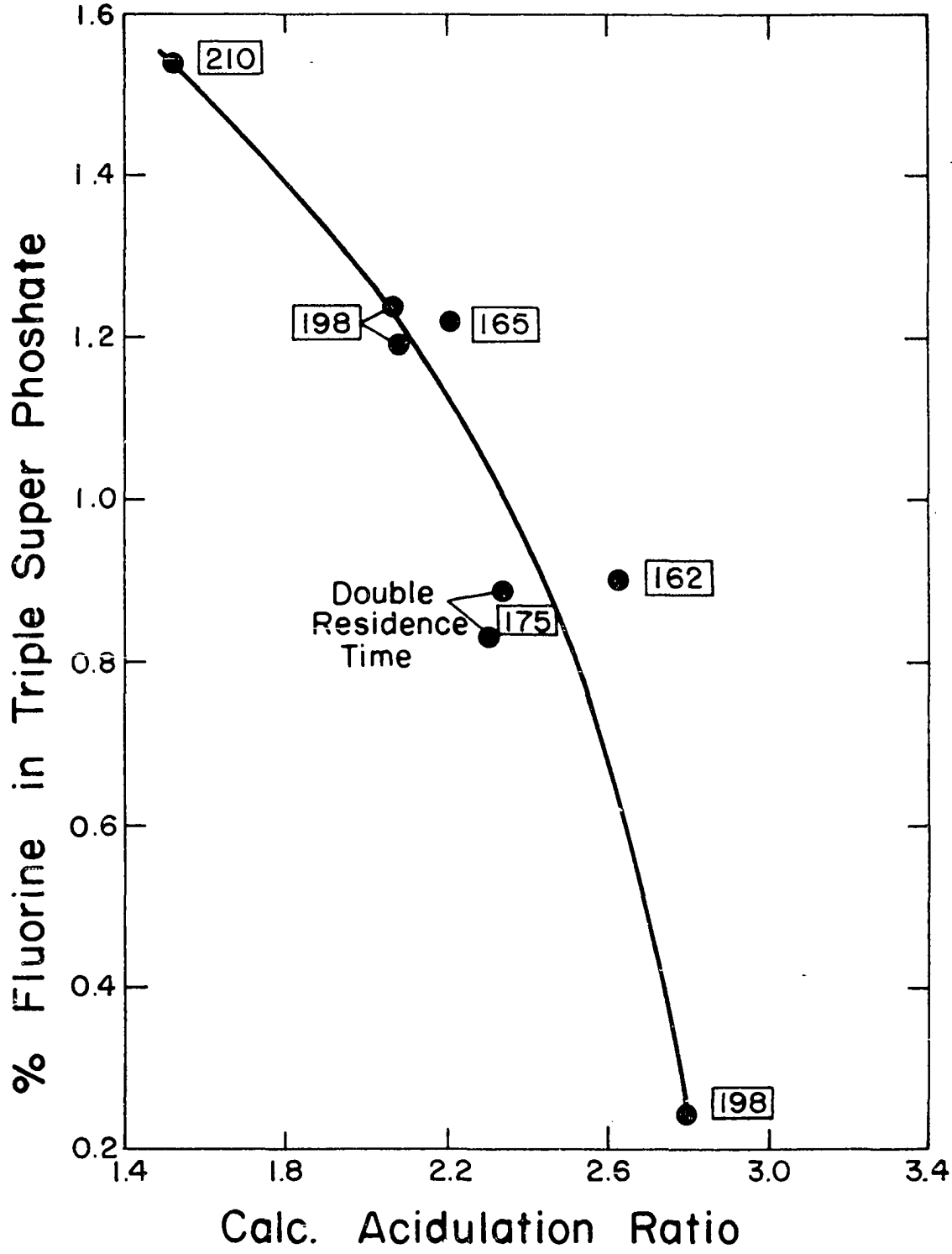
% Fluorine in Triple Super Phoshate
Calc. Acidulation Ratio
1.6
1.4
1.2
1.0
0.8
0.6
0.4
0.2
1.4
1.8
2.2
2.6
3.0
3.4
210
198
165
162
Double
Residence
Time
175
198

process. Besides, higher acidulation would guarantee complete conversion of the phosphate rock.

Monocalcium phosphate leaching

Extraction or leaching of monocalcium phosphate from the product of the first stage reaction was investigated using 5% and 10% phosphoric acid solutions as solvents. Triple-super-phosphate produced by Boylan and Amin (3) in th .r . lot plant was used. The analyses of two samples of triple super phosphate used are given in Table 9. Ten grams of triple super phosphate were weighed and 50 milliliters diluted phosphoric acid were added. The mixture was heated to a prespecified temperature, thoroughly mixed, and then allowed to settle. The solution was decanted and the solid residue was mixed with another 50 milliliters of dilute phosphoric acid and heated to the same temperature. The solution was filtered and the residue was washed with a small amount of hot water. The residue was dried, weighed and analyzed for total P_2O_5.

Figure 32 shows the effect of temperature and acid concentration on the extraction of P_2O_5 from the solids. A small amount of P_2O_5 in the residue is due to the presence of unreacted rock in the samples. These two samples had about 0.65% of citrate insoluble P_2O_5. In the proposed process, due to the use of a higher acidulation ratio, triple-super-phosphate would have almost no unreacted rock left in it and hence almost complete leaching of P_2O_5 can be expected. Moreover, leaching at a higher concentration and temperature would also assure complete recovery of P_2O_5.

Process advantages

The advantages of the rod mill for making triple-super-phosphate are:

Figure 32. P_2O_5 extraction from 10 gram triple-super-phosphate with pure phosphoric acid of 5% and 10% concentration at different temperatures

tal P_2O_5 in Residue
15
20
25
30
35
40
10%
5%
5%
0.10
0.12
0.14
0.16
0.18
of P_2O_5 in Residue, gms.

% Total P_2O_5 in Residue
0
5
10
15
20
25
30
40
50
60
70
80
Temperature C°
10%
10%
5%
5%
0.04
0.06
0.08
0.10
0.12
0.14
0.16
Wt. of P_2O_5 in Residue, gm

Table 9. Analyses of the triple-super-phosphate samples

No.	% Total P_2O_5	% Water soluble P_2O_5	% Citrate insoluble P_2O_5	% Moisture
1[a]	54.02	50.71	0.657	1.69
2[b]	53.77	51.39	0.636	3.87

[a]10 percent phosphoric acid used for leaching

[b]5 percent phosphoric acid used for leaching

1. The process is continuous and requires a short residence time (less than 2 hours) for complete conversion of rock phosphate to triple-super-phosphate (3).

2. Under the severe conditions (3) that exist inside the rod mill, most of the fluorine is driven off as SiF_4 gas, since there is not present a liquid phase in which the gas may dissolve. The absence of fluorine results in a purer product acid and also reduces corrosion and scale formation caused by the fluo-silicates. Moreover, since fluorine is removed in a single operation, the process offers an attractive economic condition for its recovery.

3. Foaming during the phosphate rock attack is not a problem (3). Foaming arises in present day processes due to the presence of carbonates, fluorine compounds, and some floatation agents that are present in the phosphate rock. The continuous action of the rods stops the formation of foam.

4. The rod mill process is flexible with respect to operating

conditions (3). Phosphoric acid concentration, temperature inside the mill and the residence time can all be adjusted to achieve complete conversion. For example, higher temperatures and longer residence times can be used if acid concentration is low. A higher acidulation ratio (defined as pounds of acid P_2O_5 per pound of rock P_2O_5) may be employed to reduce the residence time since the excess acid returns to the process. Also, the effect of variations in the rock feeding rate is reduced by a higher acidulation ratio.

5. For every 100 lbs. of rock entering the reaction mill, 78 lbs. of water are removed as vapor. In the gypsum process this water must be removed by flash evaporation, thus increasing the cost of the product acid.

6. The residue from the leaching operation was found to contain mainly silica and organic impurities. In the commercial process these organic impurities disintegrate into black coloring matter when they come in contact with sulfuric acid. Due to their small particle size, it is impractical to remove them by filtration. Thus the removal of organic matter during leaching will eliminate this difficulty, resulting in a clear phosphoric acid.

Advantages for crystallizing semihydrate are as follows:

1. The wet-process requires the removal of large amounts of water, since a large quantity of water has to be used to wash gypsum crystals (dihydrate). Also the phase relationship constraint, Figure 1, for the crystallization of gypsum, require relatively low temperature and acid concentration. The lower temperature is maintained by removing the heat

of reaction by flash evaporation.

If calcium is crystallized as semihydrate, a higher temperature, in excess of 70 C°, and a higher acid concentration, in excess of 35% P_2O_5, can be used, thus reducing the load on the flash evaporator. Although the schematic diagram of the process, Figure 30, shows a flash chamber, it is not necessary. It was incorporated to maintain a heat balance based on a crystallization temperature of 70 C°. If this temperature is increased and/or cooling by air injection is employed, then the thermal balance can be achieved without the flash chamber.

The heats of reactions used for these calculations were estimated from standard heats of formation. A 15% loss due to radiation and convection was also assumed.

2. Control of the crystallizer will be easier than that for the traditional wet-processes. Feed for the wet-processes is solid rock phosphate, whereas the proposed process utilized a liquid feed. In addition, loss of unreacted rock in waste gypsum, because of particle coating, will be completely eliminated. Also, close control of SO_4^{--} concentration in the semihydrate process is not necessary, which on the other hand, is an absolute necessity for the gypsum process. An excess of SO_4^{--} concentration in the crystallizer is maintained for the extraction of P_2O_5 from the rock particles and for the reduction of $CaHPO_4 \cdot 2H_2O$ co-crystallization in the gypsum crystal structure. Analyses of semihydrate crystals invariably showed a negligible loss of P_2O_5 due to solid solution formation. In the proposed process close control of SO_4^{--} concentration can be maintained at stoichiometric requirements, thus

resulting in a saving of raw material sulfuric acid. The reduction in SO_4^{--} concentration also results in a purer acid product.

3. Considerably higher growth rates and lower nucleation rates are obtained for semihydrate crystallization than those for gypsum system. This will result in a shorter residence time requirement for the crystallizer.

CONCLUSIONS

1. A previously developed mathematical analysis technique for a MSMPR crystallizer was found to be an excellent tool for the determination of the kinetics of nucleation and growth of calcium sulfate.

2. A laboratory scale, continuous, mixed suspension, mixed product removal crystallizer was built and operated for the reaction crystallization of calcium sulfate and was found to be a suitable laboratory device to determine the kinetics of the crystallization process.

3. Kinetic order of the reaction crystallization of calcium sulfate semihydrate from 42% P_2O_5 phosphoric acid, at 70 C° was determined. Kinetic relationship between nucleation and growth was found to be

$$\frac{dN^o}{dt} = K_1 r^{2.8} \qquad \text{for pure system}$$

and

$$\frac{dN^o}{dt} = K_1 r^{2.6} \qquad \text{for impure system} \quad .$$

4. Effect of suspension density was investigated and the experimental data were found to be in agreement with a model that indicates that homogeneous nucleation is the basic mechanism for the reaction crystallization of $CaSO_4$ as semihydrate. Higher suspension densities were found to be favorable for the production of larger crystals, but it was concluded that an upper limit existed because of practical limitations.

5. Phosphoric acid concentration has no effect on growth or nucleation in the concentration range of 49.5% to 58% phosphoric acid.

6. Temperature affects growth and nucleation rates significantly. At low temperatures growth rate decreased and nucleation rate increased. Water of crystallization also increased indicating partial transformation

of semihydrate into dihydrate (gypsum). The resulting high nucleation rate and slow growth rate for gypsum crystallization, under the conditions of lower temperatures and lower acid concentrations, limited experimental work since the crystals obtained were not suitable for Coulter Counter analysis. It was shown that semihydrate can be crystallized at a considerably higher growth rate and lower nucleation rate than gypsum.

7. A laboratory procedure showed that the size distribution analysis of calcium sulfate semihydrate crystals, almost an impossible task by traditional methods, can be achieved by the use of the Coulter Counter.

8. The atomic structure of a calcium sulfate crystal was studied and a theory was proposed for the control of the habit. This theory was experimentally tested by crystallization of semihydrate. Increase in calcium ion concentration decreased the lengths of semihydrate crystals but it also induced formation of spherulites.

9. Incorporation of phosphate ions in the crystal structure was found to be negligible.

10. A process flow-sheet and material balance were prepared for a new process. Important advantages of the new process are:

(a) almost all of the P_2O_5 in the phosphate rock can be recovered as phosphoric acid,

(b) product phosphoric acid would be much purer and clearer,

(c) corrosive fluorine compounds are removed in the first stage reaction in a single unit and can be easily recovered if desired,

(d) concentration of phosphoric acid produced is much higher and therefore an expensive evaporation process is not necessary. Acid can be directly used for triple-super-phosphate manufacture or for the purpose of ammoniation,

(e) the process can be completely automated and would require much less maintenance than the gypsum process.

RECOMMENDATIONS

1. Application of a mathematical theory of a MSMPR crystallizer should be extended to other processes (e.g. process for ammonium phosphate, potassium nitrate, ammonium sulfate, etc.).

2. Impurities have been used to control growth, nucleation and habits in a variety of commercial crystallization processes. Detailed study of their effects under different process conditions can be studied. The determination of the kinetic order can reveal the effect of impurities on nucleation. Determination of nuclei population densities and growth rates by a MSMPR crystallizer, under different conditions with and without impurities can be helpful in understanding the relationship between process variables and impurities. Therefore, effect of impurities on nucleation and growth processes should be studied using the MSMPR crystallizer model.

3. Advantages of higher suspension density in a MSMPR crystallizer have been discussed. However, the inability of the present-day techniques to dissipate the feed solutions in the suspension quickly, thus maintaining its mixed characteristics throughout the suspension, prohibits use of higher suspension densities. New techniques should be developed for introducing feeds in large size crystallizers, which would avoid localized regions of heavy supersaturation. Until then, however, all crystallization operations, where supersaturation is created by the addition of feed solutions (such as reaction crystallization) should be carried out in a number of smaller size crystallizers running in parallel. For the same residence time and production rate, two small crystallizers

in parallel would produce a better crystal distribution than one large crystallizer. Another pertinent recommendation is that the feed solutions should be divided and introduced at many different points in the crystallizers.

NOMENCLATURE

A	total crystal area, $(\text{microns})^2$
a,b,d	power constants
F	crystal production rate, gm/hr
K_A	area shape factor
K_1,K_2,K_2'	proportionality constants
K_g	proportionality constant (growth)
K_n	proportionality constant (nucleation)
L	crystal length, microns, measured along a characteristic axis
N	total number of crystals, numbers
N^o	total number of nuclei, numbers
n	total crystal population density, numbers/micron
n_o	steady state total crystal population density, numbers/micron
n_o^o	steady state total nuclei population density, numbers/micron
$\bar{n}_i$	suspension input point population density, numbers/micron/$(\text{micron})^3$
$\bar{\bar{n}}_o$	suspension output point population density, numbers/micron/$(\text{micron})^3$
$\bar{n}_s$	point crystal population density at suspension surface, numbers/micron/$(\text{micron})^3$
Q	total suspension flow rate, cubic microns/hr
r	crystal growth rate along characteristic crystal axis, microns/hr
r_o	steady state growth rate, microns/hr
S	supersaturation in solution, gm/$(\text{micron})^3$

T	residence time, hr
t	time, hr
V	total suspension volume, $(\text{micron})^3$

REFERENCES

1. Association of Official Agricultural Chemists. Official methods of analysis. The Association, Washington, D.C. 1950.

2. Baynham, J. W. and Raistrick, B. Structural and X-ray data on compounds found in fertilizers. In Sauchelli, V. Chemistry and technology of fertilizers. pp. 538-575. Reinhold Publishing Corporation, New York, New York. 1960.

3. Boylan, D. R. and Amin, A. B. A one-step continuous quick-curing triple superphosphate process employing red mill grinding. Agricultural and Food Chemistry 12:428-432. 1964.

4. Bransom, S. H., Dunning, W. J., and Millard, B. Kinetics of the crystallization in solution. I. Discussions of the Faraday Society 5:83-95. 1949.

5. Bunn, C. W. Some applications of X-ray diffraction methods in industrial chemistry. Journal of Scientific Instruments 18:72-73. 1941.

6. Burton, W. K. and Cabrera, N. Crystal growth and surface structure. Discussions of the Faraday Society 5:33-48. 1949.

7. Caspari, W. A. Calcium sulphate hemi-hydrate and the anhydrites. I. Crystallography. Proceedings of Royal Society (London) A155: 41-48. 1936.

8. Christiansen, J. A. and Nielsen, A. N. Kinetic determination of the size of the crystal germs. Acta Chemica Scandinavica 5:674-675. 1951.

9. Dahlgren, S. E. Physico chemical background of phosphoric acid manufacture by wet-process. Acta Polytechnica Scandinavica 271:1-15. 1960.

10. Davenport, J. E., Getsinger, J. G., and Caroll, F. Wet-process phosphoric acid - foam distribution of sulfuric acid. Unpublished mimeographed paper presented at American Chemical Society Meeting, New York, New York, Sept. 1963, Tennessee Valley Authority, Wilson Dam, Alabama. 1964.

11. First industrial application of I.M.I. phosphoric acid process. British Chemical Engineering 5:255. 1960.

12. Frank, F. C. The influence of dislocations on crystal growth. Discussions of the Faraday Society 5:48-54. 1949.

13. Hill, W. L. and Hendricks, S. B. Composition and properties of superphosphate. Industrial Engineering Chemistry 28:440-447. 1936.

14. Kurteva, O. I. and Brutskus, E. B. Solubility of calcium sulfate in $H_3PO_4 + H_2SO_4$ and $H_3PO_4 + H_2SiF_6$. Journal of Applied Chemistry, U.S.S.R. 34:1636-1641. 1961.

15. Larson, M. A. and Larson, K. L. Effect of impurities on crystal growth of gypsum. Unpublished typewritten report submitted to National Science Foundation, Washington, D.C., 1964. Chemical Engineering Department, Iowa State University of Science and Technology, Ames, Iowa. 1964.

16. Larson, M. A., Timm, D. C., and Wolff, P. R. Effect of suspension density on crystal size distribution. Unpublished mimeographed paper. Chemical Engineering Department, Iowa State University of Science and Technology, Ames, Iowa. 1965.

17. Legal, C. C., Jr., Prayor, J. N., Tongue, T. O., and Veltman, P. L. Phosphoric acid by the clinker process. Industrial and Engineering Chemistry 49:334-337. 1957.

18. MacLennan, G. and Beevers, C. A. The crystal structure of monocalcium phosphate monohydrate. Acta Crystallographica 9:187-190. 1956.

19. Marc, R. Über die kristallisation ans waserigen losungen. Zeitschrift für Physikaliche Chemie 67:470. 1909.

20. McCabe, W. L. Crystal growth in aqueous solutions. Industrial and Engineering Chemistry 21:112-119. 1929.

21. Murray, D. C. Size distribution dynamics in continuous crystallization. Unpublished Ph.D. thesis. Library, Iowa State University of Science and Technology, Ames, Iowa. 1964.

22. Nordengren, S. British Patent 378,670. 1931. Original not available; cited in Sauchelli V. Chemistry and Technology of fertilizers. p. 241. Reinhold Publishing Corporation, New York, New York. 1960.

23. Nordengren, S., Francia, I., and Nordengren, R. The first installation of a phosphoric acid plant according to the anhydrite method at Vercelli, Italy. Fertiliser Society (England) Proceedings 33:1-27. 1955.

24. Piombino, A. J. Phosphates. Chemical Week 95:109-132. 1964.

25. Powers, H. E. C. Macroscopic growth of crystals. Industrial Chemist 39:421-425. 1963.

26. Powers, H. E. C. Nucleation and early crystal growth. Industrial Chemist 39:351-355. 1963.

27. Randolph, A. D. The mixed suspension, mixed product removal crystallizer as a concept in crystallizer design. American Institute of Chemical Engineer's Journal 11:424-430. 1965.

28. Randolph, A. D. Size distribution dynamics in a mixed crystal suspension. Unpublished Ph.D. thesis. Library, Iowa State University of Science and Technology, Ames, Iowa. 1962.

29. Randolph, A. D. and Larson, M. A. Transient and steady state size distributions in continuous mixed suspension crystallizers. American Institute of Chemical Engineers Journal 8:639-645. 1962.

30. Saeman, W. C. Crystal size distribution in mixed suspensions. American Institute of Chemical Engineers Journal 2:107-112. 1956.

31. Sauchelli, V. Normal superphosphate: Chemistry and technology. In Sauchelli, V., ed. Chemistry and technology of fertilizers. pp. 129-166. Reinhold Publishing Corporation, New York, New York. 1960.

32. Taperova, A. A. and Shulgina, M. N. Kinetics of transformations of crystal hydrates of calcium sulfate in the presence of phosphoric acid. Journal of Applied Chemistry, U.S.S.R. 23:27-46. 1950.

33. Timm, D. C. Crystal size distribution dynamics. Unpublished Ph.D. thesis. Library, Iowa State University of Science and Technology, Ames, Iowa. 1965.

34. Verma, A. R. Crystal growth and dislocations. Butterworths Science Publications, London, England. 1953.

35. Volmer, M. Kinetic der phasenbildung. Edward Brothers, Inc., Ann Arbor, Michigan. 1945.

36. Waggaman, W. H. Phosphoric acid, phosphates, and phosphatic fertilizers. 2nd ed. Reinhold Publishing Corporation, New York, New York. 1952.

37. Weber, W. C. and Pratt, C. J. Wet-process phosphoric acid manufacture. In Sauchelli, V. Chemistry and technology of fertilizers. pp. 197-250. Reinhold Publishing Corporation, New York, New York. 1960.

ACKNOWLEDGMENTS

The author wishes to express his deep gratitude and sincere thanks to Dr. M. A. Larson for his painstaking interest and help during the course of this investigation. A word of thanks is due to Dr. D. R. Boylan who encouraged the author to pursue work in the field of fertilizer technology.

The author also wishes to thank Mr. R. T. Johnson for his assistance in the chemical analyses and Mr. D. C. Timm for his valuable assistance.

The author would like to acknowledge the Iowa Engineering Experiment Station whose facilities and resources made possible this investigation.

APPENDIX A

Supersaturation

Experimental values of supersaturation are very difficult to obtain. Supersaturation levels are generally extremely low and especially so for the cases of MSMPR crystallizers. Solubility of calcium sulfate in phosphoric acid is of a very small magnitude and it is affected by impurities. For example, it is reduced drastically by common ion effect.

One method to experimentally determine the level of supersaturation in a MSMPR crystallizer is as follows. First, a liquid-crystal slurry is removed from the crystallizer, and the crystals are immediately separated from the mother liquid, all at constant temperature. The clear liquid will adjust to the equilibrium level if it is allowed to stand for a long period of time. During this time the level of supersaturation will be depleted by further crystallization. After equilibrium conditions have been reached, the new crop of crystal are separated from the liquid, being careful to maintain constant temperature and to remove all of the liquid from the crystals. The weight of these crystals is directly related to the supersaturation level that existed in the crystallizer.

Experimentally withdrawal of sample and its subsequent separation cannot be done in zero time and therefore, results may be erroneous. However, an attempt was made to find the supersaturation for several runs. Samples were withdrawn and filtered quickly. The mother-liquor was allowed to crystallize calcium sulphate at room temperature. After 20 days this suspension was slowly heated to the original temperature of the MSMPR crystallizer from which the sample was taken. This heated

suspension was filtered to separate the crystals formed due to supersaturation. The supersaturation level was calculated as grams of calcium sulfate per gram of mother-liquor. No attempt was made to find the form of calcium sulfate crystals and it was assumed that they were semihydrate.

Knowing steady state growth rate "r" and steady state supersaturation "S", the value of constant "K_g" in the equation $r = K_g S^b$ can be found if b = 1. From the theoretical and experimental work done so far in the field of crystallization, a value of one for "b" is considered to be quite appropriate.

Experimental results and the evaluation of the constant are presented in Table 10. It can be seen from the table that supersaturation levels are quite low. The values of K_g obtained for three different runs are almost all the same. However, the actual values might be somewhat different due to the experimental errors.

Table 10. Estimation of proportionality constant K_g using growth rates and supersaturation levels

Run No.	Temp C°	Residence time T minutes	% suspension density gms./100 gms.	Growth rate r microns per hour	Super-saturation[a] S gm./gm.	$K_g = \frac{r}{S}$
35	76	38.3	3.763	84.9	4.86×10^{-4}	17.5×10^{4}
46	70	42.1	1.950	78.3	3.93×10^{-4}	19.9×10^{4}
48	70	42.1	3.760	91.0	4.58×10^{-4}	19.9×10^{4}

[a]Presented on the basis of gram per gram mother-liquor